EFFECTS OF UNCERTAINTIES IN PROBABILISTIC SEISMIC HAZARD ANALYSIS ON RESPONSE OF A TALL BUILDING

by

Oğuz Şenkardeşler

B.S., Civil Engineering, Boğaziçi University, 2013

Submitted to the Institute for Graduate Studies in
Science and Engineering in partial fulfillment of
the requirements for the degree of
Master of Science

Graduate Program in Civil Engineering

Boğaziçi University

2016

EFFECTS OF UNCERTAINTIES IN PROBABILISTIC SEISMIC HAZARD ANALYSIS ON RESPONSE OF A TALL BUILDING

APPROVED BY:

Assoc. Prof. Serdar Soyöz .....
(Thesis Supervisor)

Assist. Prof. Serdar Selamet .....

Assist. Prof. Ufuk Yazgan .....

DATE OF APPROVAL: 25.07.2016

ACKNOWLEDGEMENTS

I am grateful to my supervisor, Associate Professor Serdar Soyöz, for his guidance, encouragement and understanding throughout the preparation of this thesis. His support made it possible for me to complete this study. I would like to thank him for sharing his invaluable experience in the field of structural health monitoring and I am proud to be a member of his research group.

I am also thankful to Assistant Professor Serdar Selamet and Assistant Professor Ufuk Yazgan for their precious comments and the time they spared for my thesis.

I would like to thank to Emre Aytulun, Hüseyin Çolak and Korkut Kaynardağ for their friendship during the fieldworks, the experience we gained together are invaluable. Without their encouragement I cannot be able to finish this thesis.

I would like to express my special thanks to my colleagues Selahattin Akalp and Burak Horoz, for their vital support to shape up the structure of my thesis. I am very grateful to have such friends who do not hesitate to share their knowledge with me.

I would like to thank my brothers; Burak Atacı, Veysel Aydın, Fatih Karaca, Gökay Namlı, Talha Öğüt and Atilla Özer for their brotherhood, which helped me a lot to finish this thesis.

I would like to express my deepest gratitude to my parents and my brother. They encouraged me throughout my life and they never made me feel alone. All the things they provide me are the reason of my success and happiness.

Most of all, I would like to thank to my wife Gizem, for her incredible patience and sacrifices she made throughout the preparation of this thesis. I am very grateful to her for being my main source of motivation.

ABSTRACT

EFFECTS OF UNCERTAINTIES IN PROBABILISTIC SEISMIC HAZARD ANALYSIS ON RESPONSE OF A TALL BUILDING

Structures in seismic regions are designed to withstand the seismic demands imposed by ground motions. Design of a tall building is usually performed with an extra care due to the amount of investments done for the construction and also the possible consequences in case of an undesired structural damage. Special care is needed for the estimation of seismic demand since the design of a structure is generally governed by seismic forces in seismic-prone regions. Finite element model (FEM) of the structure is expected to fulfill the target response requirements under selected ground motions in order to satisfy the requirements of a properly designed structure. Ground motion records used in the analyses should be selected in accordance with the seismic hazard results expected at the site of the structure. Seismic hazard of a site can be determined via probabilistic seismic hazard analysis (PSHA). PSHA utilizes seismicity models and ground motion prediction equations (GMPEs) to calculate hazard levels. Seismicity models are very sensitive to uncertainties, so as the hazard levels. These uncertainties and their effects on seismic hazard estimations are investigated in this study. By conducting linear time-history analyses with the selected ground motions on a 43-story reinforced concrete tall building in Istanbul, the effects of these uncertainties on the response of a tall building is also investigated. In order to validate the FEM, structure is instrumented with accelerometers and system identification (SID) is conducted with ambient vibration measurements. In addition to the seismic hazard calculations, structural models have uncertainties as well due to the assumptions and subjective decisions in modeling phase. It is crucial to validate the FEM or update the FEM according to SID results in order to catch a realistic behavior of the real structure.

ÖZET

OLASILIKSAL SİSMİK TEHLİKE ANALİZİNDEKİ BELİRSİZLİKLERİN YÜKSEK BİR YAPININ TEPKİSİNE ETKİSİ

Sismik bölgelerdeki yapılar yer hareketlerinden kaynaklanan sismik taleplere dayanabilecek şekilde tasarlanırlar. İnşaat için yapılan yatırım ve istenmeyen yapısal hasar durumunda oluşabilecek sonuçlar sebebi ile yüksek yapıların tasarımı genellikle ekstra bir dikkat ile yapılır. Sismik istemin tahmin edilmesi de özel bir dikkat ile yapılması gerekir çünkü, sismik bölgelerde binaların tasarımı genellikle sismik kuvvetler tarafından belirlenir. Yapının düzgün tasarlanmış bina gereksinimlerini sağlayabilmesi için, yapının sonlu elemanlar modelinin seçilen yer hareketi kayıtları altında hedeflenen tepki gereksinimlerini yerine getirebilmesi gereklidir. Analizlerde kullanılacak yer hareketi kayıtlarını, yapının olduğu bölgede beklenen sismik tehlike sonuçlarına göre seçilmesi gereklidir. Bir bölgenin sismik tehlikesi olasılıksal sismik tehlike analizi (OSTA) ile belirlenebilir. OSTA tehlike seviyesini belirlemek için depremsellik modelleri ve yer hareketi tahmin denklemlerinden yararlanır. Depremsellik modelleri belirsizliklere karşı çok hassastır, dolayısı ile tehlike seviyeleri de böyledir. Bu çalışmada, bu belirsizlikler ve bunların sismik tehlike tahminlerine olan etkisi incelenmiştir. Seçilen yer hareketi kayıtları ile İstanbul'da bulunan 43 katlı betonarme yüksek yapı üzerinde zaman tanım alanında doğrusal analizler yapılarak, bu belirsizliklerin yüksek yapının tepkisine olan etkisi de incelenmiştir. Sonlu elemanlar modelinin doğrulanması için binaya ivme sensörleri yerleştirilmiş ve ortam titreşimi ölçümleri ile sistem tanımlanması yapılmıştır. Sismik tehlike hesaplarına ek olarak, yapı modellerinde de modelleme esnasında yapılan varsayımlardan dolayı bir belirsizlik vardır. Sonlu elemanlar modelinin doğrulanması veya sistem tanımlama sonuçlarına göre güncellenmesi mevcut yapının gerçekçi davranışının yakalanması için çok önemlidir.

TABLE OF CONTENTS

LIST OF FIGURES

LIST OF TABLES

LIST OF SYMBOLS

a	The number of earthquakes occurred in a period larger than minimum considered magnitude
b	Ratio of large earthquakes to small earthquakes
E_c	Elastic modulus of concrete
EI	Flexural rigidity
f	Frequency
f_c	Compressive strength of concrete
k	Spring coefficient
M	Earthquake magnitude
m_{min}	Minimum magnitude considered
$N_{m>M}$	Number of earthquakes with magnitude larger than M
T	Structural period
T_1	Fundamental mode period
V_{s30}	Average shear wave velocity at upper 30m of soil
β	b*ln(10)
ε	"epsilon" , a quantity which measures the difference between the record's spectral acceleration and mean spectral acceleration estimate of ground motion prediction equation at a specific period
μ	Mean
σ	Standard deviation

LIST OF ACRONYMS/ABBREVIATIONS

ACI	American Concrete Institute
ASCE	American Society of Civil Engineers
BA2008	Boore and Atkinson (2008)
CB2008	Campbell and Bozorgnia (2008)
CY2008	Chiou and Youngs (2008)
DSHA	Deterministic Seismic Hazard Analysis
EFDD	Enhanced Frequency Domain Decomposition
EMA	Experimental Modal Analysis
ERA	Eigensystem Realization Algorithm
FDD	Frequency Domain Decomposition
FEM	Finite Element Model
FFT	Fast Fourier Transform
GMPE	Ground Motion Prediction Equation
GR	Gutenberg and Richter
IDA	Incremental Dynamic Analysis
IDR	Inter-storey Drift Ratio
IM	Intensity Measure
MAC	Modal Assurance Criterion
MSE	Mean Square Error
NAF	North Anatolian Fault
NAFZ	North Anatolian Fault Zone
NEHRP	National Earthquake Hazards Reduction Program
NExT	Natural Excitation Technique
NGA	Next Generation Attenuation
N4SID	Numerical Algorithm for Subspace State-Space System Identification
PGA	Peak Ground Acceleration
PSHA	Probabilistic Seismic Hazard Analysis
PSD	Power Spectral Density

RETMC	Regional Earthquake-Tsunami Monitoring Center
RO	Reverse-Oblique
SA	Spectral Acceleration
SF	Scale Factor
SID	System Identification
SRSS	Square Root of Sum of Squares
SS	Strike-Slip
SSI	Stochastic Subspace Identification
TSC	Turkish Seismic Code
TS	Turkish Standards
UDIM	Uluslararasi Deprem Izleme Merkezi
UHS	Uniform Hazard Spectrum
3-D	Three directional

1. INTRODUCTION

1.1. Overview

Earthquake is one of the most important and challenging phenomena in civil engineering field. Its significance arises from the effect of its tremors on structures and the unpredictability of its nature forms the challenging part. Damages induced to structures by earthquakes may result in intolerable economic losses and even worse; loss of lives in case of collapse. Especially in earthquake prone areas, design procedures of buildings are highly dominated by seismic loads. Magnitude of the seismic loads may vary from site to site and determined via seismic hazard analyses.

Seismic hazard analyses are carried out by using either deterministic or probabilistic approaches, or both. Deterministic seismic hazard analysis (DSHA) considers the design earthquake as the largest earthquake that a source is likely to generate and it happens at the closest point of the fault to the site. Since there is a relation between the magnitudes of earthquakes and their recurrence periods (Gutenberg and Richter, 1944) and the location of the earthquake is almost impossible to predict, deterministic seismic hazard analysis seems to consider worst-case scenario only, and not the real situation. On the other hand, probabilistic seismic hazard analysis (PSHA) aims to take magnitude and distance uncertainties of the earthquakes into account. PSHA is a better representation of the reality in many cases; therefore, results obtained from PSHA can be more reliable.

Besides the differences given above, both methods are pretty much the same. The effect of design earthquake at a specific site is obtained by utilizing ground motion prediction equations (GMPEs). There are a lot of GMPEs derived for different tectonic regimes, soil types and etc. Recurrence period of earthquakes also may be calculated with different earthquake magnitude-frequency distributions (recurrence models) which plays a crucial role in hazard results. In order to estimate the recurrence period of an earthquake, properties of the fault should be known. Since recurrence periods for

earthquakes are long, the compiled information on faults, so far, is limited. Additionally, especially for the recently urbanized areas, the required information is even more limited.

All of these approximations done in order to cope with these uncertainties make seismic hazard analysis subjective. Depending on the methods used, approximations made, results may differ from analyst to analyst. Engineering judgment and experience become important at this point. The main objective of this study is to present the sensitivity of the results of PSHA and the response of a tall structure to the choices made during probabilistic seismic analyses. Moreover, the effect of uncertainties related to GMPE selection and magnitude-frequency distribution of PSHA in response of a structure was also investigated. A 43-story reinforced concrete tall building was modeled and the earthquake records selected according to PSHA results. Under selected records linear time-history analyses were conducted and inter-story drifts were investigated as a response parameter. In order to validate the accuracy of the model, and to guide future studies, the structure was instrumented with acceleration sensors and system identification of structure was also conducted.

1.2. Literature Review

Literature review is arranged such that, first of all research of various authors about seismic hazard assessments performed for Marmara region are summarized. After that studies about uncertainties affecting the results of probabilistic seismic hazard assessment, which is adopted in this thesis, are presented. Finally research about system identification, modeling of high rise structures and model updating of finite element models are presented.

1.2.1. Literature Review on Seismic Hazard Analysis

Erdik *et al.*, (2004) presents a fault segmentation model for Marmara Region. All seismicity parameters for segmentation model are determined by authors and several probabilistic seismic hazard analyses are conducted. Time-dependent (Poisson) and

time-independent (renewal) models are constructed and compared via seismic hazard maps. Since Kocaeli and Duzce earthquakes hit the eastern part of the region five years before this paper and the fault beneath the Marmara Sea is quiet since 1766, renewal model yields 2-3 times lower hazard values for eastern parts and 10 to 30% higher hazards for western parts. In this study, effect of possible cascading scenario is also investigated. Two different cascading scenarios are considered. Results for cascading scenarios are given for renewal model only. It is stated that the cascading effect may increase the hazard values up to 50% for extreme cases and for most of the Istanbul City increase is about 10 to 20%.

Kalkan *et al.*, (2009) reassessed probabilistic seismic hazard of Marmara Region at the time. Their model consists of two source models; smoothed-gridded seismicity model and fault model. Earthquakes with a magnitude between 4 and 6.5 are modeled with smoothed-gridded seismicity and, earthquakes with a magnitude greater than 6.5 are modeled with faults. All seismicity parameters were obtained by authors from an earthquake catalogue, whose completeness and declustering are done by the authors again. They used a logic-tree in order to consider the uncertainties. One regional and three next-generation attenuation (NGA) GMPEs are employed in the study and weights of them are adjusted in logic-tree such that regional GMPE has a weight of 0.5 and others share the remaining equally. Fault model is modeled with two recurrence models (based on Gutenberg-Richter recurrence law and characteristic earthquake) and the results are combined with equal weights. Maximum magnitude that faults can produce is also accounted in logic tree. Mean estimate of Wells and Coppersmith (1994) has a weight of 0.6 and mean ± 1 sigma cases have 0.2 each. In the end results are presented for Marmara Region as maps, and it is emphasized that the values increased 10 to 15% with respect to the values used at the time.

Gülkan (2012) presents the results of a seismic hazard assessment of Istanbul with a deterministic approach. Study considers six possible deterministic earthquake scenarios. Those scenarios include individual or multiple rupturing of submarine faults passing through the north of Marmara Sea, which is the western part of North Anatolian Fault Zone. In order to include epistemic uncertainty, author employed six

different GMPEs. In order to eliminate the subjectivity of the weighting in logic-tree approach, relative success of GMPEs performance in predicting the observed motions of the 1999 Kocaeli earthquake is used for weighting purposes. Weights of each GMPE are adjusted according to their accuracy in spectral acceleration (SA) estimations for each period separately. Site specific seismic hazard maps for peak ground acceleration (PGA) are also presented in paper for six different scenarios. PGA and SA values computed at center points of each district of Istanbul and total population and the population density for these districts are also provided in the paper.

Porter *et al.*, (2002) investigates the sensitivity of the damage on the structures to major uncertain variables. Authors consider variables such as assembly capacity, spectral acceleration, ground motion record, damping, mass and etc. Variable of interest is changed between 10th and 90th percentile while others are kept at their best estimates, and analyses are conducted for each set in order to determine the damage factor. 20 ground motion records are selected and scaled according to their spectral accelerations at natural frequency of model. Model is analyzed under these records to observe record-to-record variability. A record is scaled for different spectral accelerations and all scaled records of that record are used in analyses to observe the effect of spectral acceleration level. It is stated that the assembly capacity is the most effective variable in damage factor and the second effective variable is spectral acceleration. Record-to-record variation comes after these two variables.

Yunatci and Cetin (2006) carried out a parametric study to emphasize the effect of aleatory variability and epistemic uncertainty about GMPEs. PSHA was conducted for four sites with different distances to the source in Bursa, Turkey, and results were compared for different GMPE's with and without aleatory variability (standard deviation) inclusion. Four different GMPE were used in analyses and results showed that hazard values for zero aleatory variability may differ by a factor of more than 1.5. According to this study inclusion of aleatory variability may increase the hazard values by more than a factor of two. In some extreme cases values increases three times.

Cramer *et al.*, (1996) carried out a parametric sensitivity analysis for PSHA for southern California using a Monte Carlo approach. In study, three discrete, six continuous variables were selected as parameters. Discrete variables were GMPE, magnitude-frequency distribution type and blind fault inclusion or exclusion, whereas, six continuous variables were maximum magnitude, β value, shear modulus, fault length, width and slip rate. Range for continuous variable selection was ± 2 standard deviation and they took the values from different studies. According to the study, uncertainty of PSHA is highly dominated by, maximum magnitude, GMPE selection, slip rate of faults considered and magnitude-frequency distribution selected for model. Overall uncertainty was also calculated according to another reference study and it is mentioned that overall uncertainty is about $\pm 50\%$.

There is a debate in PSHA applications about including aleatory variability in GMPEs. Bommer and Abrahamson (2006), suggest including aleatory variability in GMPEs by using $\mu+3\sigma$, whereas, McGuire *et al.*, (2005) present advantages of using mean seismic hazard. Former states that, values increase significantly by including σ in calculations, especially for highly seismic zones. Difference between mean and the mean plus n-sigma (n is a positive number) become very large for long return periods. Return periods used for very important structures such as nuclear power plants, dams etc. may be 10000 years, and this increase in hazard become critical for such structures. Latter one states that according to PSHA theory using mean seismic hazard is the convenient way for PSHA.

Effects of seismicity models, parameters and GMPEs on a seismic hazard assessment are presented in Atkinson and Goda (2011), for four Canadian cities. In the light of new findings and studies they revised slip rates and etc. about sources and they employed new GMPEs in PSHA. They compared the results with the seismic hazard maps which were being used at that time. They also presented the impact of GMPE selection. They also modify source characterization for some regions. As a result, they stated that GMPE selection plays a significant role for seismic hazard values for all regions, values may differ up to a factor of two in some cases. Seismicity parameters have an important effect on hazard levels in low-to-moderate seismic regions. All mod-

ifications together result in significant differences with respect to the seismic hazard maps for that time. Those differences are not in same trend, for some regions or some spectral acceleration, values decrease; but for others, values increase.

Baker and Cornell (2005) suggest a vector-valued ground motion intensity measure which consists of spectral acceleration and epsilon (ε). Study states that epsilon has a significant ability to predict structural response. ε is a quantity which measures the difference between the record's spectral acceleration and mean spectral acceleration estimate of ground motion prediction equation at a specific period. ε is related with spectral shape by its definition, this is why it is successful at predicting structural response. Drift hazard levels are considered as structural response in study and, authors mentioned that neglecting ε value of a record while selection nearly always results in over-estimation of the mean annual rates of exceeding large drift levels. It is also stated that matching all desired parameters simultaneously may be challenging due to insufficient number of earthquake records and for this situation magnitude and distance ranges may be relaxed in order to match ε values of records during input selection.

Goulet *et al.*, (2007) presents a performance-based earthquake engineering methodology for four-story reinforced concrete building. Probabilistic seismic hazard analysis is conducted and records are selected accordingly. Two sets of input ground motions are selected for seven hazard levels. One of the sets takes ε into account, whereas other set does not. These set of records are utilized in determining the collapse capacities of structure with the help of Incremental Dynamic Analysis (IDA) method. ε is related with spectral shape of a record and it is stated in Baker and Cornell (2006) that, effect of considering ε in input selection is significant. Goulet *et al.*, (2007) mentions that if ε had been neglected while the record selection, collapse capacities obtained from IDA would be reduced 20-40%, which increases mean annual return of collapse by a factor of 5-10. Effect of using an arbitrary component or the horizontal component that first causes collapse, is also investigated. According to this study, using critical horizontal component may result in 30%lower median collapse capacity.

Jalayer *et al.*, (2010) presents a study about effect of structural modeling uncertainties on seismic assessment of reinforced concrete structure. Two different source of uncertainty are considered and they are mechanical properties of construction materials and reinforcement details. Lognormal distribution for mechanical properties and discrete probabilities for detailing uncertainties are utilized, and with Monte-Carlo Simulations pushover curves are obtained for each realization. Effect of using the information obtained from destructive and non-destructive test results on uncertainties considered and demand to capacity ratios are presented.

1.2.2. Literature Review on System Identification and Modeling

Brownjohn *et al.*, (2000) presents the dynamic characteristics of a 66 story high-rise building obtained from finite element models (FEM) and field measurements. Seven different models were constructed with different approaches, and their results in terms of mode frequencies and mode shapes were compared with the results obtained from field measurements. Structure was instrumented and from ambient acceleration measurements mode frequencies and mode shapes were extracted. Fourier spectra were used for identification of mode frequencies. Different modeling approaches include stick model, neglecting all openings, neglecting small openings, including all openings, including thin walls, excluding outriggers and only core-wall model. Model which was the most detailed one was in the best match with field measurements. It is mentioned in the study that, openings has the strongest influence on torsional behavior. Moreover, outriggers in some storys of the structure have a significant effect on fundamental translational mode.

Ventura *et al.*, (2005) conducted system identification and finite element model updating for two different structures. These structures are 15-story and 48-story reinforced concrete structures. Ambient measurements were taken and the experimental modal analyses (EMA) were conducted for both structures. An automated FEM updating was also conducted for those structures. Two software packages were utilized during this study, ARTeMIS and FEMTools. Those software packages are capable of extracting natural frequencies and mode shapes of structures from ambient vibration

measurement via output-only system identification methods, such as frequency domain decomposition method. Packages are also able to update FEMs by changing selected parameters. This selection was done according to a sensitivity analysis conducted by the authors. Initial parameters were Young's Modulus of element types or element types at specific regions, mass density of same elements, moment of inertia of same elements and thickness of cladding for this study. Those initial parameters, that will be included to sensitivity analysis, are selected with engineering judgment. FEM updating is conducted with the parameters that are proved to be effective at the modal analysis results. Software packages find best parameters set according to differences between experimental and analytical natural frequencies, and modal assurance criterion (MAC) value of the analytical mode shapes. It is emphasized in the paper that, at the end of analyses it is up to the analyst to accept the changes suggested by the program and to justify how realistic are the changes to be done.

Skolnik *et al.*, (2007) presents the system identification and model updating procedure for a 15-story steel structure. Preliminary prediction of dynamic modal properties is done by Fast Fourier Transform (FFT) method applied to acceleration response of structure to a small earthquake and ambient vibrations. Numerical Algorithm for Subspace State-Space System Identification (N4SID) is employed for further analyses. According to identified modal properties under earthquake excitation, they updated their model with a simple "stick" model. Stick model has mass; translational and torsional effective stiffness at each story and alters the behavior of the structure.

Moaveni *et al.*, (2007) investigated the performance of three output-only system identification techniques, namely Natural Excitation Technique combined with Eigensystem Realization Algorithm (NExT-ERA), Stochastic Subspace Identification (SSI) and Enhanced Frequency Domain Decomposition (EFDD). Methods were investigated using acceleration responses taken from both full-scale structure and its finite element model. Structure utilized in this study was a 7-story slice of a structure, including shear wall, floors and gravity columns. Structure was located on a shake table. Three output-only methods were subjected to a sensitivity analysis by the authors with parameters; excitation amplitude, spatial density of sensors, noise level and length of

measurements. It is stated in the paper that excitation amplitude has a significant effect on estimating natural frequencies for all methods considered.

1.3. Objective

Seismic hazard analysis is a very important tool in determining the seismic demands, especially in earthquake prone regions such as Istanbul, California and Tokyo, which are usually obtained from seismic hazard analysis results. By using the seismic hazard analyses, uniform hazard spectrum (UHS) can be obtained for specific sites and return periods. For different return periods, uniform hazard spectra are constructed and each UHS is used at different stages of design according to importance of the structure and/or decision makers' expectations. From UHSs, intensity measures such as peak ground acceleration (PGA), short and long period spectral accelerations may be taken and used to construct design spectra to be used in response spectrum analysis etc. or UHSs may be directly utilized to select ground motion records to be used in linear or non-linear time history analyses. Seismic hazard analysis involves substantial amount of uncertainties and assumptions in it. Every parameter used and every assumption made affects intensity measure levels. Almost all parameters and assumptions used are open for discussions. Each one of them can be considered as a different research topic and there are already a lot of studies about them (Bommer and Abrahamson, 2006; McGuire *et al.*, 2005; Atkinson and Goda, 2011). Therefore this study aims to emphasize the sensitivity of PSHA to the parameters and uncertainties, and also the effects of different seismic hazard levels to input ground motion record selection and drift response of a tall structure.

Effects of some properties such as GMPE selection and recurrence model selection are further investigated. By using combinations of two recurrence models (Gutenberg-Richter recurrence law (GR) and characteristic earthquake) and three GMPEs (Boore and Atkinson, 2008; Campbell and Bozorgnia, 2008; Chiou and Youngs, 2008), six different sub-models are constructed. Uniform hazard spectra are obtained from each and seven ground motion records are selected and scaled in order to make them compatible with the uniform hazard spectra.

Total of 42 ground motion records are utilized for linear time-history analyses of a detailed finite element model of 43-story reinforced concrete structure in Istanbul, Turkey. Modeling of the beams and columns of the structure are done by using frame elements whereas reinforced concrete core and slabs of the building are modeled using shell elements. Responses under 42 different earthquake records are compared in terms of inter-story drift ratios in order to show the correlation of uncertainties of input selection with response of the structure.

Verification of the structural model is done by system identification technique (frequency domain decomposition, FDD). The structure is instrumented with acceleration sensors and data recorded are analyzed using FDD technique. Finite element model (FEM) updating is not performed due to the good match between the behavior of FEM and the real structure. Instrumentation will be used for long-term monitoring of the structure for future studies.

1.4. Scope

Both the outline and summary of the thesis are provided in this chapter. Chapter 1 consists of overview in which the topic of the thesis is briefly described, literature review, and objective of the thesis where the topic is described more in details and the scope part.

In chapter 2, brief information on the seismotectonics of Marmara region is given and then the PSHA methodology is described combined with its parameters, sensitivity analysis of the PSHA in terms of UHS. Chapter 2 also describes the uniform hazard spectra. In the end of this chapter, deaggregation of the hazard results and the ground motion record selection and scaling according to deaggregation results are also presented.

Chapter 3 walks through the general information about structure, finite element modeling phase and dynamic characteristics of the structure.

In Chapter 4, information about validation of the FEM, in addition to instrumentation and the system identification of the structure are explained.

In chapter 5, linear elastic responses of structural model obtained from linear time-history analyses under 42 different earthquake records are presented.

In chapter 6, summary of the results, comments, conclusion and brief information about future studies is explained.

2. PROBABILISTIC SEISMIC HAZARD ANALYSIS

2.1. Methodology

Seismic demand calculation is a crucial part of the earthquake resistant design. Seismic demand on a structure depends on the dynamic characteristics of the structure, the seismic hazard of the site where the structure is located, and the soil type of the site. The soil type effect is out of scope of this study. Seismic hazard is a site-dependent phenomenon, that's why it is calculated for each project separately or seismic hazard maps are constructed for a region. As it is mentioned in former chapters, those calculations can be carried out in different ways. First way is to determine a worst case scenario. Possible maximum magnitude-minimum distance pairs are determined from accounted faults. In other words for each fault that can affect the site, maximum magnitude and the closest distance to the site are considered. Worst case scenario is selected among those magnitude-distance pairs. Since this method considers only single magnitude and single distance, which is not the case in reality, it is called deterministic seismic hazard analysis (DSHA). The other way is probabilistic seismic hazard analysis (PSHA) which considers all possible magnitudes and all possible locations of earthquakes with their occurrence probabilities. PSHA methodology is utilized throughout this thesis and described in this part of Chapter 2.

Sources in PSHA can be classified in three types. These source types are called point, line and area sources. Line and area sources are used in this thesis. Earthquakes can be divided into two groups as large and other earthquakes. The term "large" here, is a subjective term. Earthquakes with magnitudes greater then a specific value may be considered as a large earthquake. When the distribution of these large earthquakes is investigated it can be seen that these earthquakes are more likely to occur on or around faults. Smaller earthquakes are observed to happen more scattered. In the light of this information, line sources or narrow area sources are defined to represent the effect of large earthquakes, whereas smaller earthquakes are usually modeled as area sources.

Characterization of those sources is performed based on research about seismotectonics of the region. Fault lines or areas are defined according to the historical background of regions. Distribution of earthquakes is plotted on the map of region of interest, and then according to trends of recurrence characteristics of earthquakes, areas and/or lines are defined. Since there is a relation between the rupture lengths and energy releases (i.e. magnitudes) at earthquake events, lengths of line sources and areas of area sources should be consistent with the maximum magnitude earthquake observed in that region. This relation is introduced by Wells and Coppersmith (1994). Earthquakes may occur anywhere on the defined line sources or area sources in accordance with their magnitudes. For instance, smaller earthquakes may occur almost everywhere on the sources, but larger earthquakes are more likely to be around the middle of the faults. This situation is about the rupture length-magnitude relation again. In order to generate largest possible earthquake, fault should rupture completely. Measuring the distance is another issue. There are different types of minimum distance definitions which will be defined in coming chapters. All of these possibilities constitute the distance uncertainty of PSHA and the probability density function of focal distance in Figure 2.1.

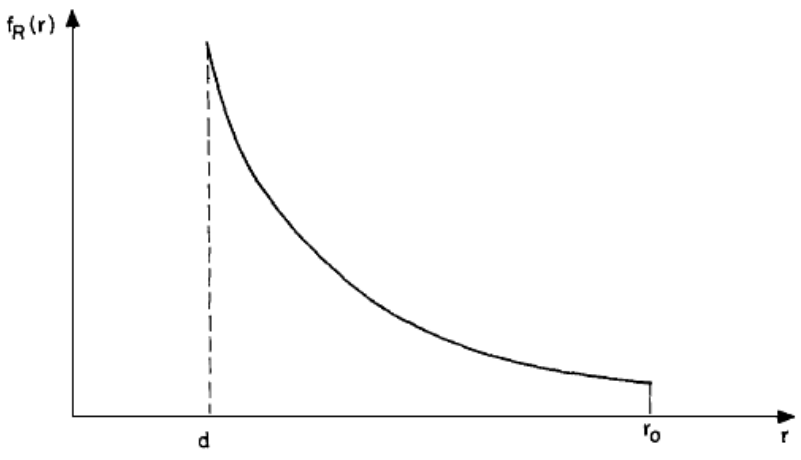

Figure 2.1. Probability density function of closest distance.

The next uncertainty is about the magnitude of the earthquake. As one may expect smaller earthquakes are more likely to occur than the larger ones. Gutenberg

and Richter (1944) indicates that, there is a logarithmic relation (Equation 2.1) between the numbers of earthquakes occurred larger than a magnitude and the magnitude.

$$\log(N_{m>M}) = a - bM \tag{2.1}$$

where "a" is the number of earthquakes occurred in a period larger than minimum considered magnitude, "b" is the ratio of large earthquakes to smaller earthquakes, "N" being the number of earthquakes larger than the variable M (the magnitude).

This relation is called Gutenberg-Richter recurrence law. Depending on the "a" and "b" values in Equation 2.1, line defined by this equation sometimes goes through the unrealistic earthquake magnitudes for the fault considered (i.e 8 or 9 magnitudes). Gutenberg-Richter relation is often bounded with a maximum magnitude as a remedy to this defect (Figure 2.2). Gutenberg-Richter assumes Poisson distribution for earth-

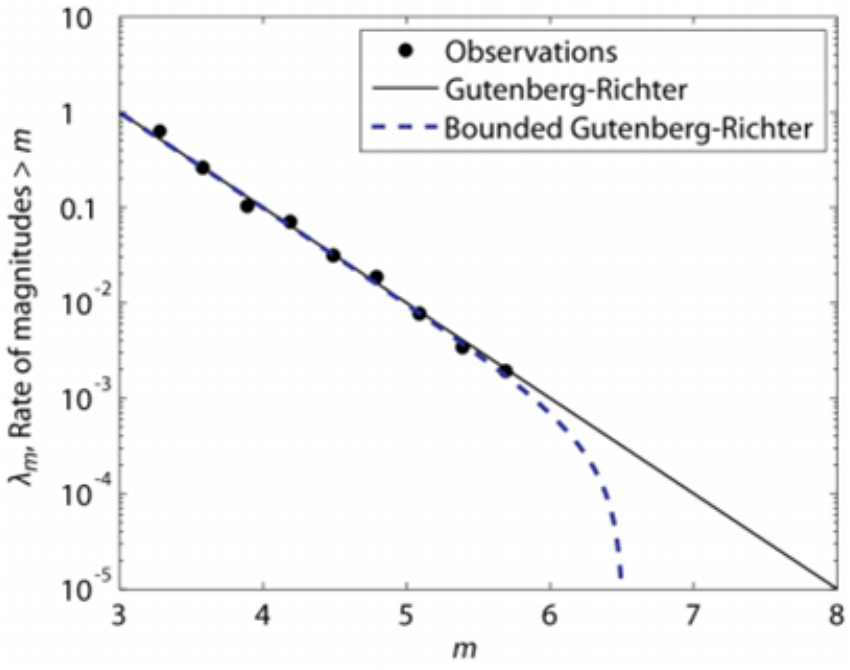

Figure 2.2. Observations, Gutenberg – Richter and Bounded Gutenberg – Richter recurrence laws (Baker, 2008).

quakes, which means earthquake events are independent from each other. Moreover, there is no time-dependence for earthquake occurrences (memoryless model). There are also time-dependent (renewal models) models using log-normal or other distributions in which the probability of an occurrence is obtained according to last earthquake occurred. Those models are out of the scope of this thesis. Another research presented in Schwartz and Coppersmith (1984) shows that larger earthquakes occur more frequently than the Gutenberg-Richter estimates (Figure 2.3). The magnitude of earthquakes that the deviation observed is called characteristic magnitude. This model is applicable for only well-defined faults.

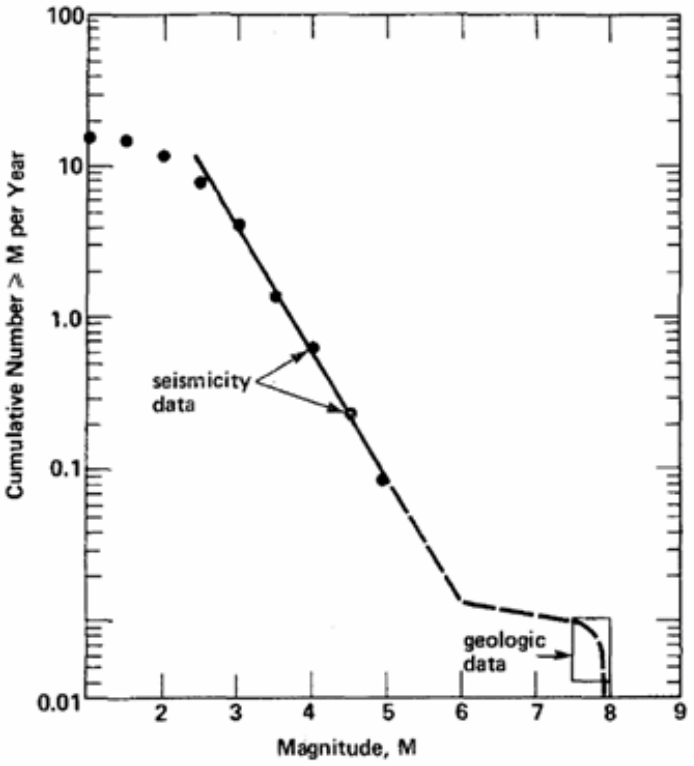

Figure 2.3. Characteristic earthquake definition (Youngs and Coppersmith, 1985).

In order to obtain the constants "a" and "b" defined by Gutenberg-Richter recurrence law, historical background of the region should be known. The perfection of the relation can only be achieved by perfect knowledge about historical background which is not easy to obtain. Knowledge about earthquakes' magnitudes and locations are

relatively better for the instrumented period. Before the instrumented period, since there was no instruments to measure magnitudes and to specify the location of earthquakes, only limited information about large earthquakes are available. Information mentioned here is not exact. Only some information about earthquakes that affected big cities is found from written literature. According to these sources the magnitude of the earthquake and the location is predicted from the damages observed in cities in those years. Since the population was sparse in rural areas, locations of earthquakes occurred in those years are not reliable.

Earthquake catalogues are compiled with that information and a completeness test is applied to catalogue which is introduced by Stepp (1973). As a result, this method determines the reliability of the catalogue for each magnitude bin. In other words, method specifies the reliable range of years for specific earthquake magnitudes. Completeness year for larger earthquakes are much longer than moderate or small earthquakes as expected.

Weichert (1980) suggested a method for obtaining Gutenberg-Richter (GR) parameters from catalogues with considering the completeness. Since the after-shocks (and foreshocks) and main-shocks are dependent, including after-shocks to catalogues violates the Poissonian distribution assumption of earthquake occurences, therefore including aftershocks to catalogue may lead to miscalculations of GR parameters. Therefore, before obtaining those parameters, catalogues should be filtered in order to discard aftershocks or foreshocks. This filtering procedure is called declustering. Different declustering methods are proposed by Gardner and Knophoff (1974), Reasenberg (1985) and etc. Once the declustering is completed, more realistic GR parameters can be obtained and the uncertainties due to the magnitude-frequency distribution can be handled.

Since the distance probability, $f_R(r|m)$, and the magnitude probability, $f_M(m)$, are independent variables, joint probability can be calculated easily as in Equation 2.2.

$$\lambda(IM > x) = \lambda(M > m_{min}) \int_{m_{min}}^{m_{max}} \int_{r_{min}}^{r_{max}} P(IM > x|m,r) f_M(m) f_R(r|m) dr dm \quad (2.2)$$

where $P(IM > x|m,r)$ term is coming from GMPE. For all distance and magnitude pairs, selected GMPEs are employed to find the intensity measure at a site. Results coming from each pair are mean values of intensity measure predicted. Knowing the mean value and the standard deviation for selected GMPE, exceedance probability can be obtained. Exceedance probabilities for each magnitude-distance pair are summed and finally the value multiplied with the rate of occurrences of earthquake greater than a minimum magnitude, $\lambda(M > m_{min})$. Final result represents the seismic hazard of that site for a specific intensity measure such as peak ground acceleration, spectral acceleration at a specific period and etc. (Figure 2.4). This analysis is conducted for every source that can affect the site and in the end hazard quantities are summed as presented in Figure 2.5.

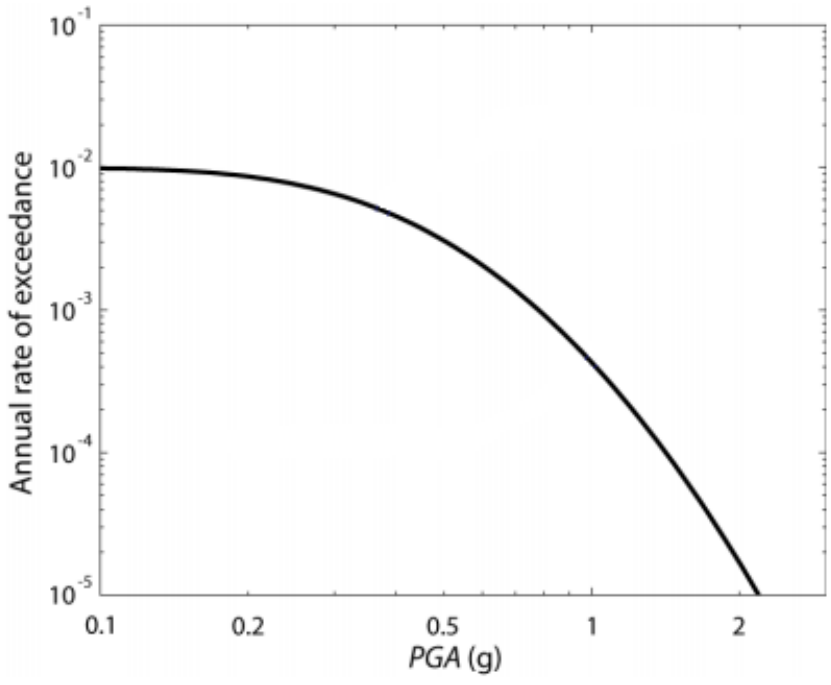

Figure 2.4. Probabilistic seismic hazard curve of a single source (Baker, 2008).

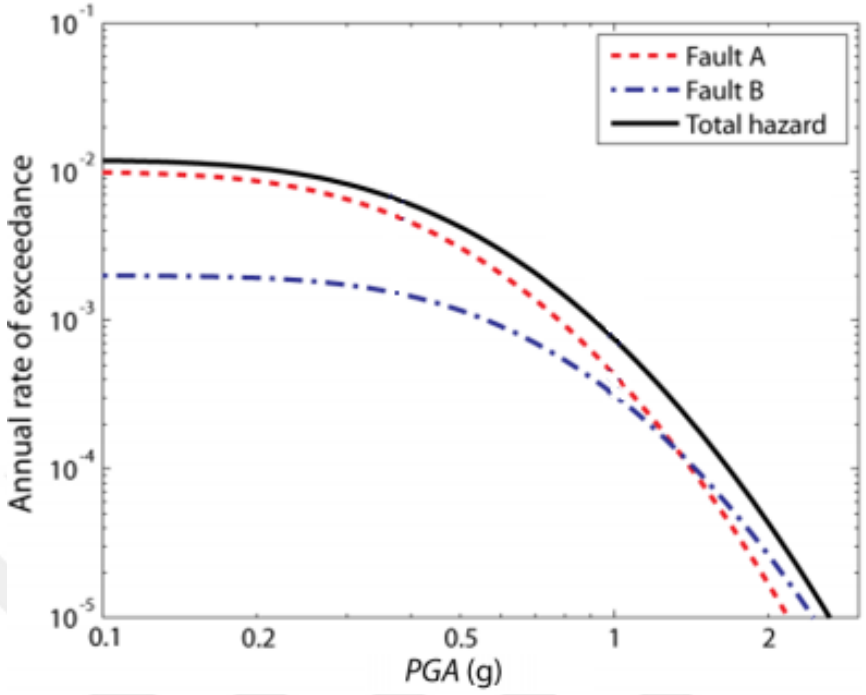

Figure 2.5. Probabilistic seismic hazard curve for two source site (Baker, 2008).

Another way to present the seismic hazard is plotting uniform hazard spectrum (UHS). UHS is plotted with data taken from several seismic hazard curves. As it is mentioned before, seismic hazard curves are calculated for a specific intensity measure (i.e. SA(T=t) or PGA). Presenting results not for a specific intensity measure but only for fixed annual rate of exceedance value, can be more useful for an engineer. Seismic hazard analyses are conducted for many different intensity measures and from each curve values are obtained for a fixed annual rate of exceedance. All data are plotted on a period vs. spectral acceleration graph and the curve that formed is UHS. UHS looks like design spectrum, this is why it is more meaningful for engineers (Figure 2.6).

The selection of this GMPE itself is a significant uncertainty. Moreover, each GMPE already has its own uncertainty due to regression analyses done during the derivation processes. There is a controversy about how to treat those uncertainties in a specific GMPE among the PSHA peer.

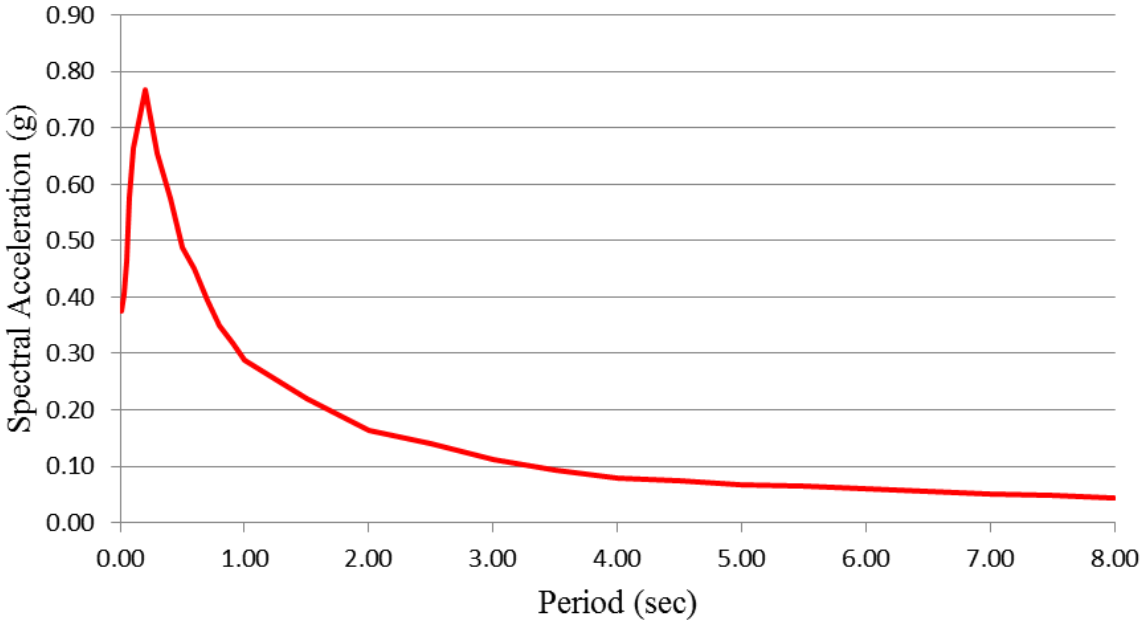

Figure 2.6. Uniform hazard spectrum (UHS).

2.2. Seismotectonics of Marmara Region

Marmara region is one of the most tectonically active regions of Turkey. Western part of North Anatolian Fault Zone (NAFZ), which extends through the northern part of the Turkey, divided into two branches and submerges to the Marmara Sea (Smith *et al.*, 1995; Parke *et al.*, 1999). Northern branch passes 15 - 20km away from the shore of Istanbul's most populated areas. Southern branch passes between Yalova and Bursa, and continues through the southern shore of Marmara Sea. Almost all faults in this area are right-lateral strike-slip faults. There are so many smaller faults around the northern branch of NAFZ below Marmara Sea. Anatolian plate rotates counter-clockwise and moves to west according to stable Eurasian plate, which results in 22±3 mm/yr right-lateral slip (McClusky *et al.*, 2000).

2.3. PSHA of the Site

In this chapter application of PSHA to the project site is described. Site studied in this thesis is located in Levent, which is a highly commercial zone of Istanbul. Levent is positioned between the first and second Bosporus bridges. Soil type of the site is assumed to be between B/C classes according to NEHRP soil classification. The location of the site is indicated in Figure 2.7. For the PSHA of the site, two different models are used. Models are generated with the help of computer software, CRISIS (M. Ordaz *et al.*). In models line faults are assumed to be at depth of 12km, and area sources are modeled at 10km. Depth become important at distance measurements. GMPEs utilize different type of closest distance definitions. Some of the GMPEs use distance between the rupture and the site whereas others use surface projection of the rupture and the site. This is the part where depth gets into calculations. Another issue about distance is about, which point on the rupture is used for distance measurements. Some of GMPEs use focus point of the rupture, and some others use closest distance on whole rupture surface and etc. Among the GMPEs utilized in this thesis, Boore and Atkinson (2008) uses the shortest distance between the surface projection rupture surface and the site, whereas Campbell and Bozorgnia (2008) and Chiou and Youngs (2008) uses shortest distance between rupture surface and the site.

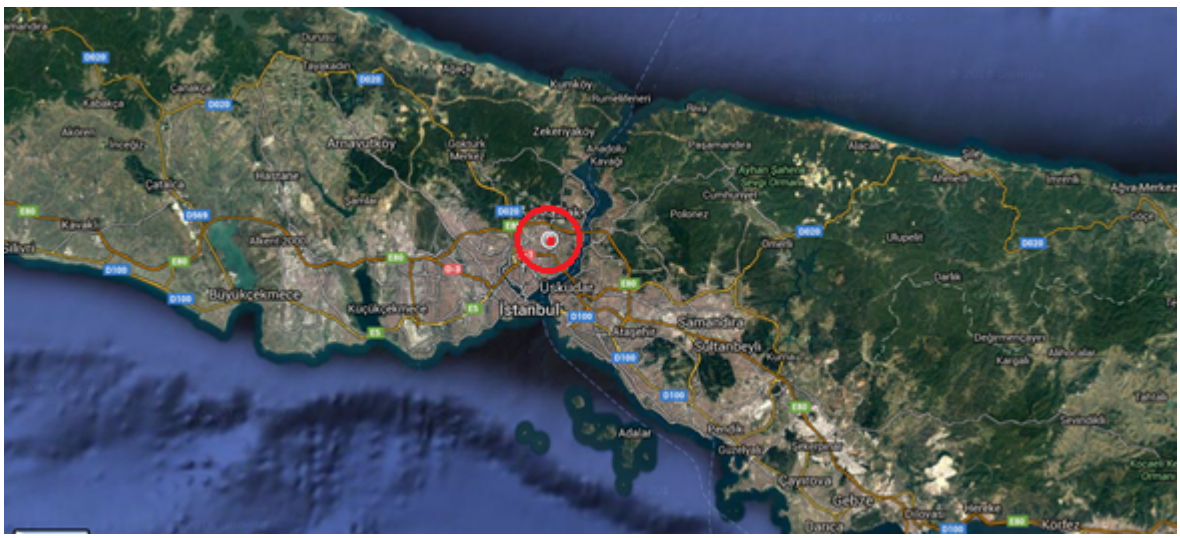

Figure 2.7. Location of the site.

Average shear wave velocity at the upper 30m of the soil (Vs30) is assumed to be 760m/s for GMPE calculations. GMPEs are employed by the software with the embedded coefficients and relations for each of them. Faults are defined by their coordinates, and their seismicity is taken into consideration with the recurrence parameters determined or adopted from studies. Software performs probabilistic seismic hazard of sites which are defined by the user for desired spectral acceleration values. For all sites of interest deaggregation is also performed by the software. Software is capable of combining different models via logic-tree approach. This logic-tree approach is not used in this study for the purpose of this thesis, which is emphasizing the uncertainties in modeling.

2.3.1. Model 1

Fault segmentation for Model 1 is taken from Erdik *et al.*, (2004), and given in Figure 2.8 Line sources and area sources are used for large and other earthquakes, respectively. Characteristic magnitude distribution is utilized for line sources whereas for area sources bounded Gutenberg-Richter distribution is used. Characteristic magnitudes for each segment and the recurrence times are directly taken from the aforementioned research. On the other hand, Gutenberg-Richter parameters for area sources are obtained from a raw catalogues taken from Regional Earthquake-Tsunami Monitoring Center (RETMC) database. Marmara Region is divided into three parts. First part does not include faults but includes north of the NAFZ, second part involves the faults of the NAFZ, and the last part is consisting of southern branch of NAFZ and the southern part of Marmara Sea. Distribution of the earthquakes larger then magnitude 4 and the three regions used for catalogue compilation is given in Figure 2.9. Earthquakes occurred between 1900 and 2015 are included to the catalogue which has a lower-bound magnitude of 4, and the GR parameters for each zone are calculated by simply fitting a line to the seismicity data. Parameters used for modeling sources are given in Table 2.1 and Table 2.2.

Three next generation attenuations (NGA) are used as GMPE. In order to show the effect of GMPE selection, they are not combined with logic-tree method which is

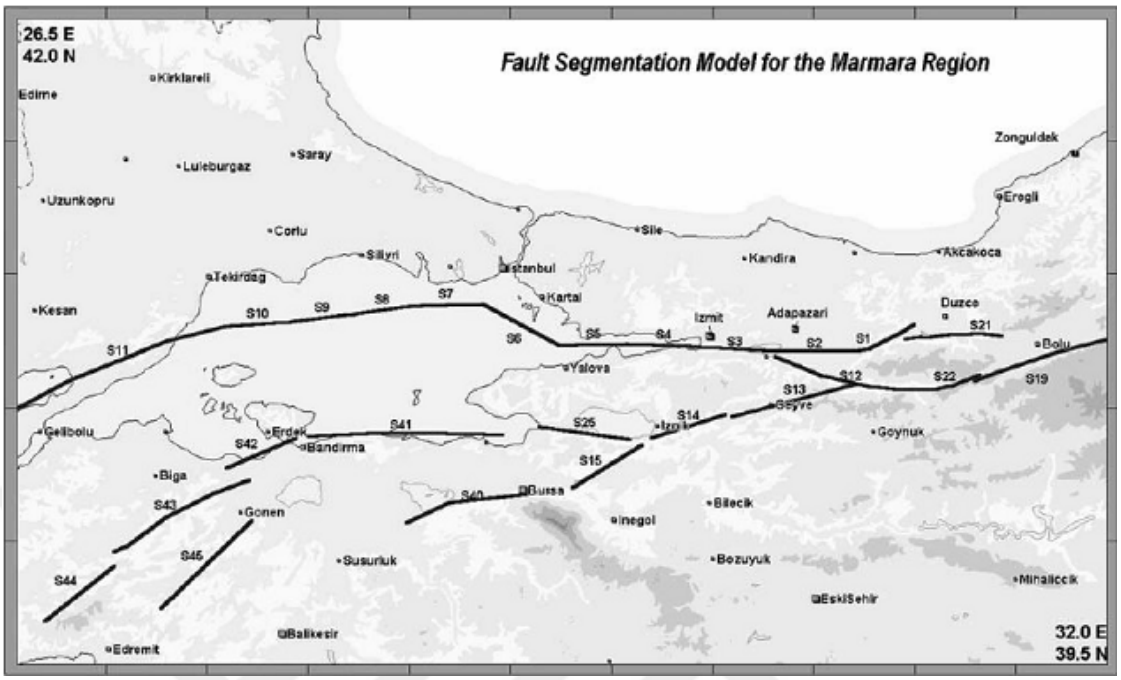

Figure 2.8. Fault segmentation model proposed by Erdik *et al.*, (2004) for the Marmara Region.

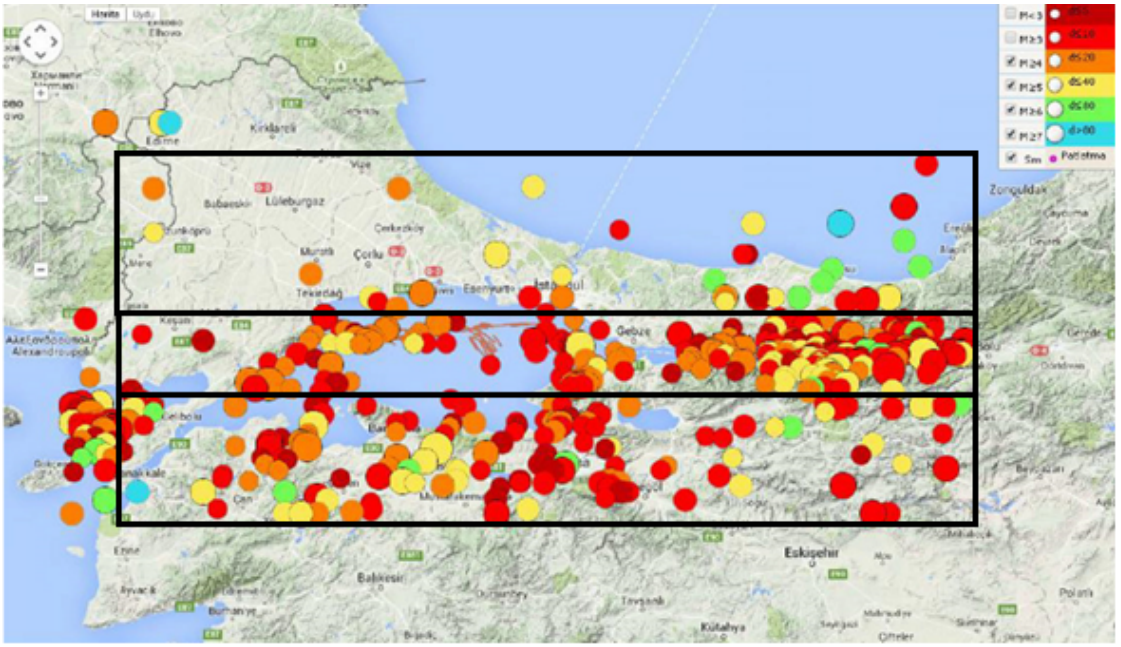

Figure 2.9. Distribution of earthquakes bigger than 4 magnitude and the regions defined for catalogue compilation.

Table 2.1. GR and other parameters for Model 1.

	a	**b**	**Min. Magnitude**	**Max. Magnitude**
Istanbul	2.17	0.741	4.0	5.5
NAFZ	3.73	0.912	4.0	7.0
Southern	3.61	0.840	4.0	6.0

the very common application among PSHA experts. Logic-trees are used in order to quantify the epistemic uncertainty by adjusting different weights to different models according to the reliability of models in expert's point of view. In this thesis Boore and Atkinson (2008), Campbell and Bozorgnia (2008) and Chiou and Youngs (2008) attenuations are employed. These attenuations will be referred as BA2008, CB2008 and CY2008 in the rest of the thesis.

Table 2.2. Parameters for linear faults, Model 1 (Erdik *et al.*, 2004).

Segment	**Recurrence time(years)**	**Char. mag.**	**Annual rate (1/year)**
S1	140	7.2	0.0071
S2	140	7.2	0.0071
S3	140	7.2	0.0071
S4	140	7.2	0.0071
S5	175	7.2	0.0057
S6	210	7.2	0.0048
S7	250	7.2	0.0040
S8	250	7.2	0.0040
S9	200	7.2	0.0050
S10	200	7.2	0.0050
S11	150	7.5	0.0067

Figure 2.10 shows the UHS's for three different return periods (72,475 and 2475 years) for BA2008 GMPE as an example. Since linear time-history analyses are carried out in following sections of the thesis, rest of the results are compared in terms of 475 years return period only which is generally used for preliminary analysis and/or checking sufficiency of serviceability target requirements of a structure.

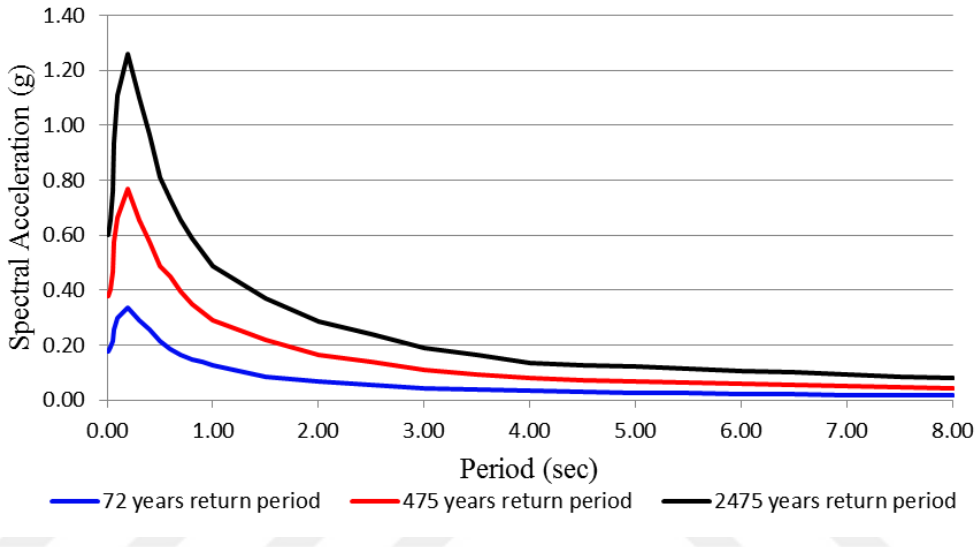

Figure 2.10. Uniform hazard spectra for three different return periods (72, 475 and 2475 years).

Figure 2.11 shows 475 years return period uniform hazard spectra for each GMPE for Model 1. It is clear that CY2008 estimates larger PGA and short period spectral accelerations. Above 4 second periods results are converging to each other. This result may mean that especially for buildings with short fundamental periods, selection of GMPE may be very critical. Design spectra in design codes usually defined according to 0.2s and 1.0s spectral accelerations. For both periods different GMPE's yield significant differences, which makes GMPE selection very critical for seismic hazard analyses. Normalized values are also given in Table 2.3 for PGA, 0.2s, 1.0s and 4.0s period spectral accelerations in order to emphasize the differences. Values in the table are normalized to the GMPE which yields smallest PGA value. 4s period spectral acceleration is also added to the table because, as it will described in following section,

building constructed on this site has a fundamental periods of 4.17s and 3.30s in X and Y directions according to finite element model, respectively.

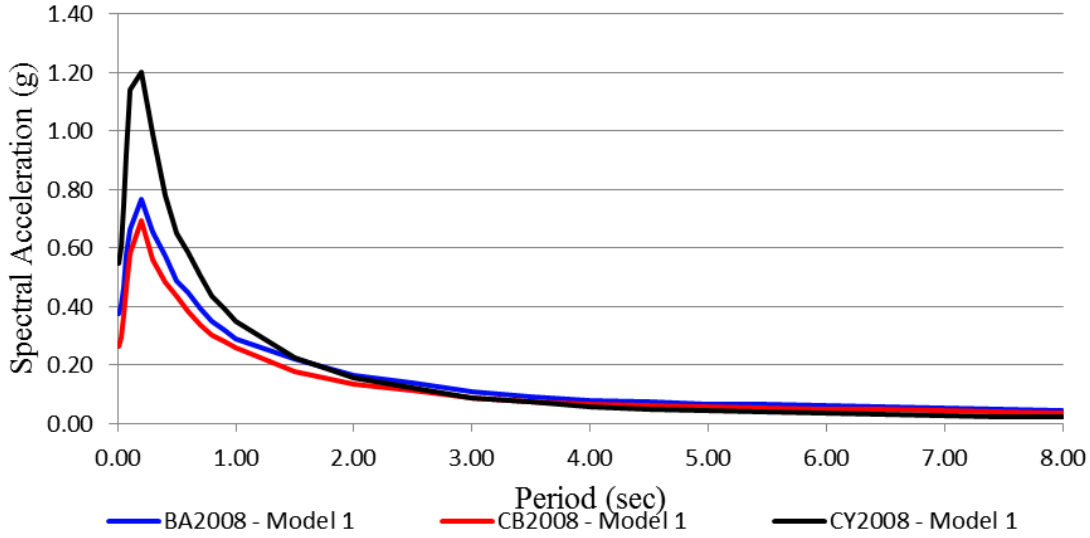

Figure 2.11. 475 years return period uniform hazard spectra for three different GMPEs (BA2008, CB2008, CY2008).

Table 2.3. Summary of results for Model 1.

	BA2008		**CB2008**		**CY2008**	
	Actual (g)	**Normalized**	**Actual (g)**	**Normalized**	**Actual (g)**	**Normalized**
PGA	0.38	1.46	0.26	1.00	0.55	2.11
T=0.2s	0.77	1.11	0.69	1.00	1.20	1.74
T=1.0s	0.29	1.11	0.26	1.00	0.35	1.35
T=4.0s	0.08	1.33	0.06	1.00	0.06	1.00

2.3.2. Model 2

Differences between second model and first model are the source model and the magnitude-frequency distribution used for large earthquakes. Characteristic earthquake model was used in first model, whereas in this model bounded GR recurrence

law is used for all earthquakes. This model also uses line sources for big earthquakes and area sources for smaller earthquakes. Line source for this model is not divided into segments but modeled as a single line source. Around this line source there is an area source which represents smaller earthquakes. There is no other area sources defined for Istanbul region and for southern parts of Marmara Sea as in Model 1, but there is a background seismicity defined for whole map, which is defined as area source again. All the parameters used, and the fault geometry are taken from Demircioğlu (2010) and they are given in Table 2.4 and in Figure 2.12 (and Figure 2.13), respectively. Fault segmentation model proposed by Demircioğlu (2010) for Turkey is given in Figure 2.14.

Same GMPEs are used for this model also for consistency. UHSs are given in Figure 2.15 and Table 2.5 is given again for comparison.

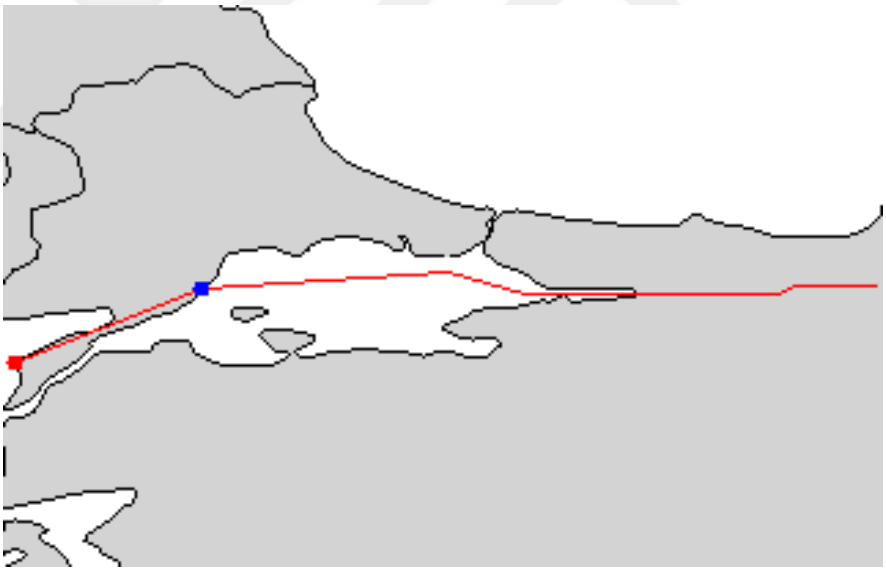

Figure 2.12. Line fault modeled in Model 2.

2.3.3. Model 1 vs. Model 2

Selection of model used in seismic hazard may also be a source of uncertainty. Therefore in this section for all GMPEs considered, two models are compared with figures and tables with actual and normalized values again.

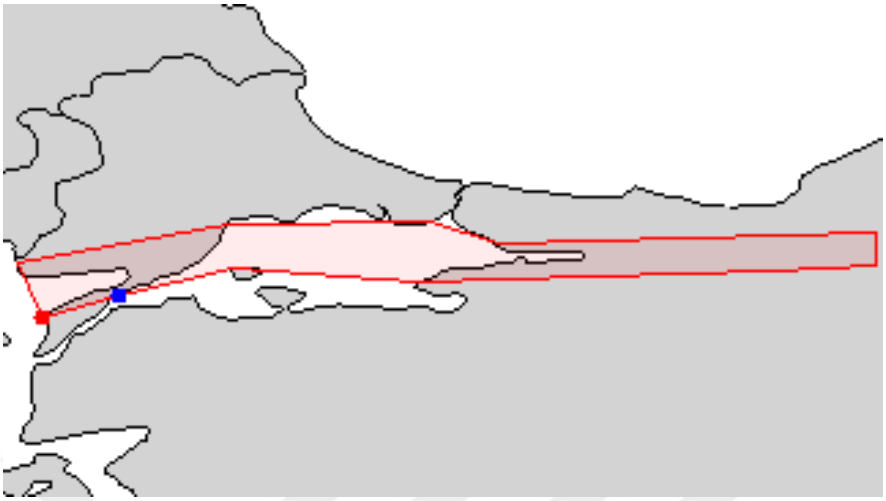

Figure 2.13. Area source modeled in Model 2.

Table 2.4. GR and other parameters for Model 2 (Demircioglu, 2010).

	a	b	Min. Magnitude	Max. Magnitude
NAFZ line soruce	5.30	0.9	7.0	7.9
NAFZ area source	5.30	0.9	5.0	6.9
Background	5.13	1.0	5.0	6.5

Table 2.5. Summary of results for Model 2.

	BA2008		CB2008		CY2008	
	Actual (g)	Normalized	Actual (g)	Normalized	Actual (g)	Normalized
PGA	0.42	1.31	0.32	1.00	0.64	2.00
T=0.2s	0.94	1.08	0.87	1.00	1.39	1.60
T=1.0s	0.34	1.17	0.29	1.00	0.40	1.38
T=4.0s	0.09	1.29	0.07	1.00	0.07	1.00

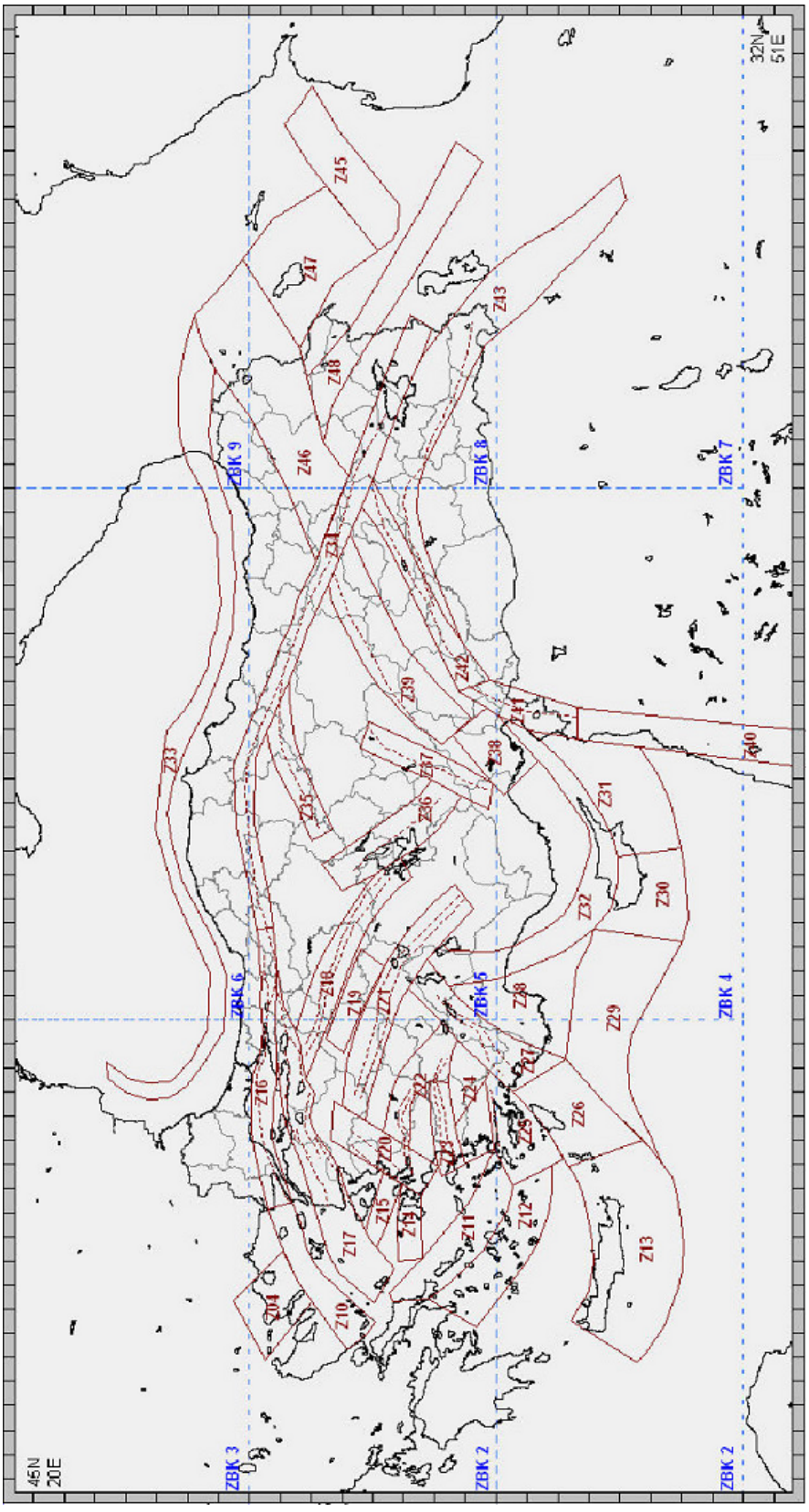

Figure 2.14. Fault segmentation model proposed by Demircioğlu (2010)

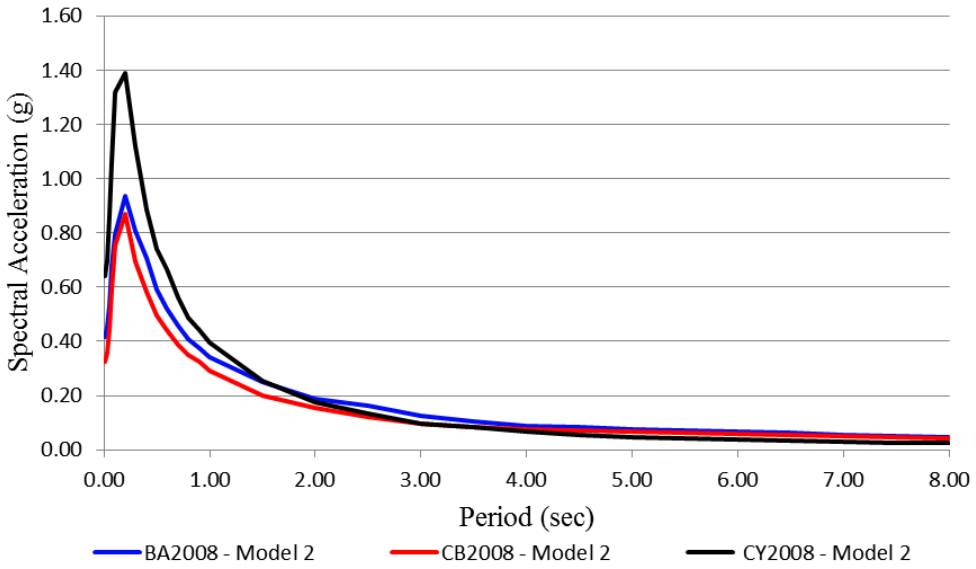

Figure 2.15. 475 years return period uniform hazard spectra for three different GMPEs (BA2008, CB2008, CY2008).

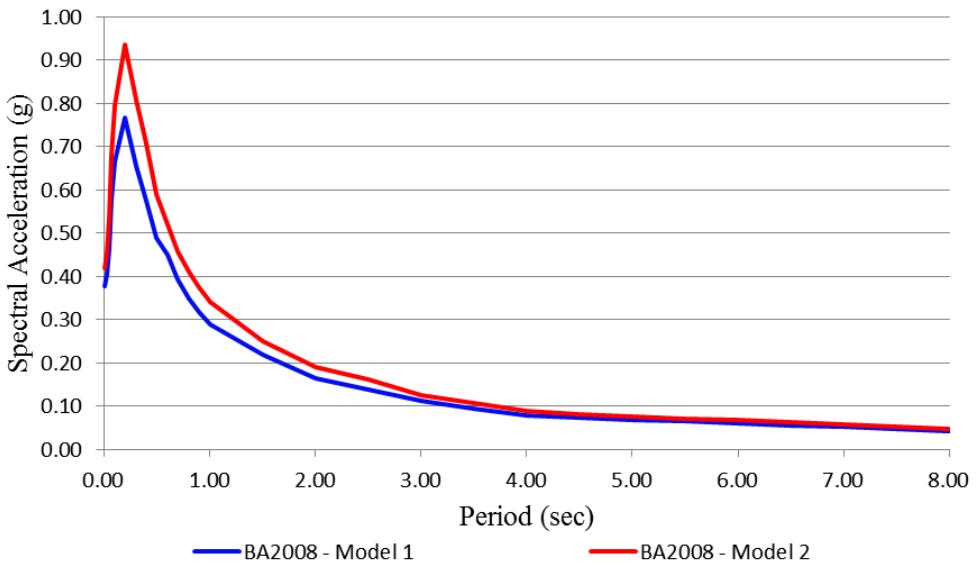

Figure 2.16. 475 years return period uniform hazard spectra for Model 1 and Model 2 (BA2008).

Table 2.6. Summary of results for Model 1 and Model 2 (BA2008).

	Model 1		Model 2	
	Actual (g)	**Normalized**	**Actual (g)**	**Normalized**
PGA	0.38	1.00	0.42	1.10
T=0.2s	0.77	1.00	0.94	1.22
T=1.0s	0.29	1.00	0.34	1.17
T=4.0s	0.08	1.00	0.09	1.12

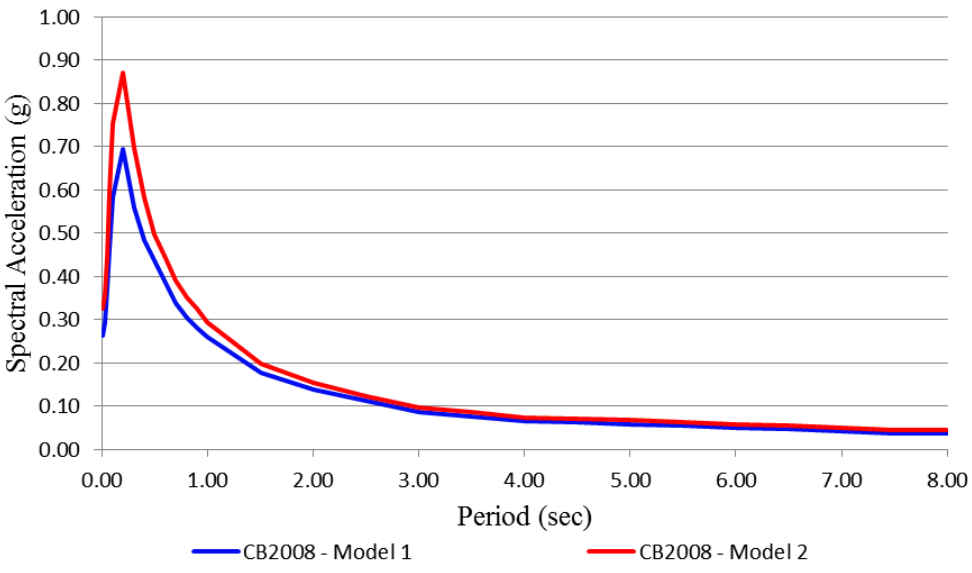

Figure 2.17. 475 years return period uniform hazard spectra for Model 1 and Model 2 (CB2008).

Table 2.7. Summary of results for Model 1 and Model 2 (CB2008).

	Model 1		Model 2	
	Actual (g)	**Normalized**	**Actual (g)**	**Normalized**
PGA	0.26	1.00	0.32	1.23
T=0.2s	0.69	1.00	0.87	1.26
T=1.0s	0.26	1.00	0.29	1.11
T=4.0s	0.06	1.00	0.07	1.17

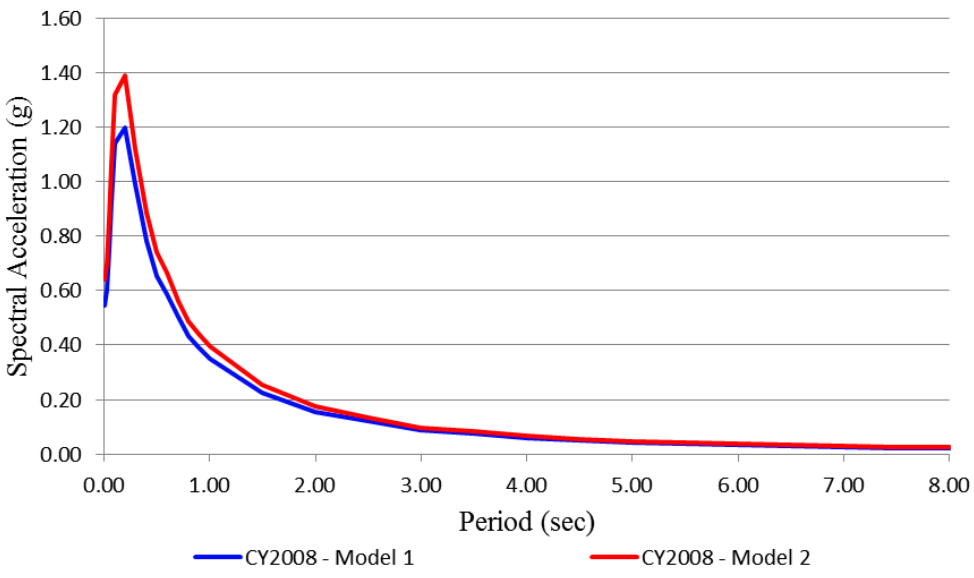

Figure 2.18. 475 years return period uniform hazard spectra for Model 1 and Model 2 (CY2008).

Table 2.8. Summary of results for Model 1 and Model 2 (CY2008).

	Model 1		**Model 2**	
	Actual (g)	**Normalized**	**Actual (g)**	**Normalized**
PGA	0.55	1.00	0.64	1.16
T=0.2s	1.20	1.00	1.39	1.16
T=1.0s	0.35	1.00	0.40	1.14
T=4.0s	0.06	1.00	0.07	1.17

2.3.4. Total Uncertainty Range Due to Recurrence Models & GMPE Selection

All choices during the PSHA effects the results as discussed in previous sections. UHS results of all sub-models and their mean are presented in Figure 2.19. This graph is plotted in order to show how the results can differ according to choices made during the PSHA. If a logic tree with equal weights was used in this thesis, mean value in the Figure 2.19 would be the result. Summary of results for all sub-models are also given in Table 2.9.

Table 2.9. Summary of results for all submodels (units in g).

	BA2008		**CB2008**		**CY2008**		**Mean**
	Model 1	**Model 2**	**Model 1**	**Model 2**	**Model 1**	**Model 2**	
PGA	0.38	0.42	0.26	0.32	0.55	0.64	0.43
T=0.2s	0.77	0.94	0.69	0.87	1.20	1.39	0.98
T=1.0s	0.29	0.34	0.26	0.29	0.35	0.40	0.32
T=4.0s	0.08	0.09	0.06	0.07	0.06	0.07	0.07

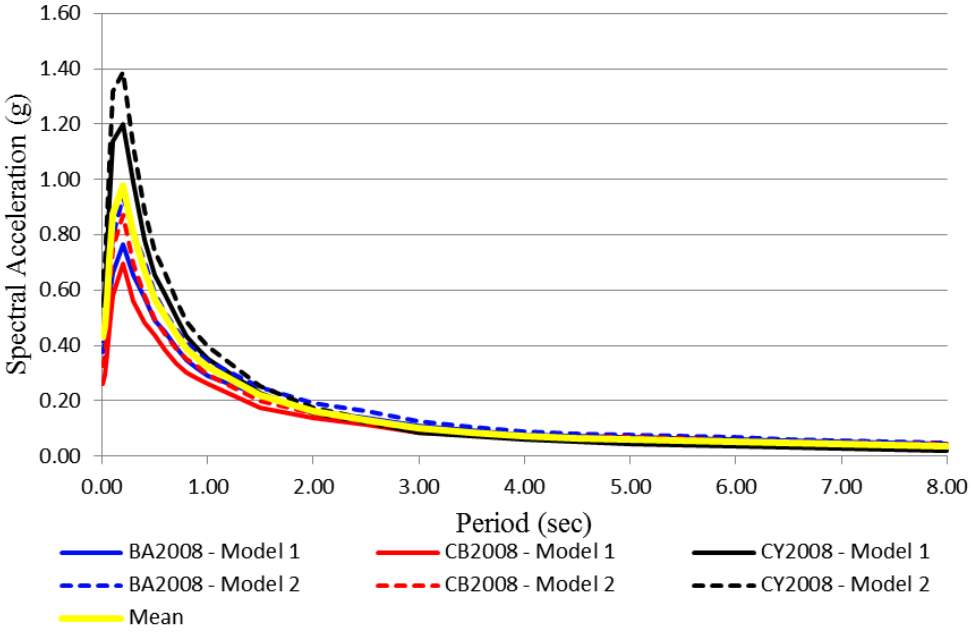

Figure 2.19. 475 years return period uniform hazard spectra for all sub-models.

2.4. Deaggregation

All sources on a model have their own distance and magnitude probabilities in a probabilistic seismic hazard analysis. When the hazards for all possible magnitudes and distances are considered and accumulated, the total seismic hazard due to that specific fault is obtained. Each magnitude and distance pair (M, R) has a contribution to total seismic hazard due to the possibility of occurrence of an earthquake with a magnitude m=M at a distance of r=R. When the sum of seismic hazard contributions from all sources having individual M&R pairs are divided by the total seismic hazard for all possible m and r values, the cumulative contribution of earthquakes with the individual M&R pairs are obtained. This method is called deaggregation and it is first suggested by Bazzurro and Cornell (1999). Since probabilistic seismic hazard analysis calculates a combined probability, deaggregation method is utilized in order to find the most contributing magnitude and distance. By doing this the most critical fault and the event can be defined. This result can be used in selecting ground motion records with magnitudes and distances compatible with the most critical case.

Since the structure considered in this thesis has a fundamental period of 4.17 seconds, in this study disaggregation procedure for SA(T=4s) for 475 years return period is applied implicitly with software. Deaggregation is performed separately for Model 1 and Model 2 for three GMPEs, six times. Results are given in Figures 2.20 to Figure 2.25 Results show similar distributions for different GMPEs. Deaggregation results of Model 1 indicate that contribution is dominated by a single magnitude bin, whereas this is not the case for Model 2. This may be due to the characteristic earthquake assumption of Model 1.

According to the distribution of contributions, ground motion records were selected separately for each submodel's deaggregation result.

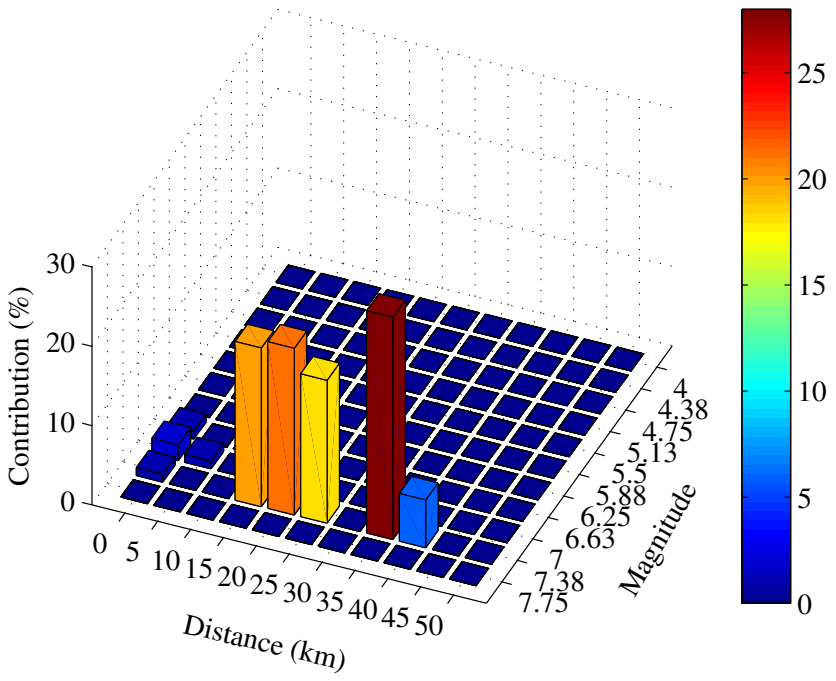

Figure 2.20. Deaggregation results for SA(T=4s), 475 years return period (Model 1 – BA2008).

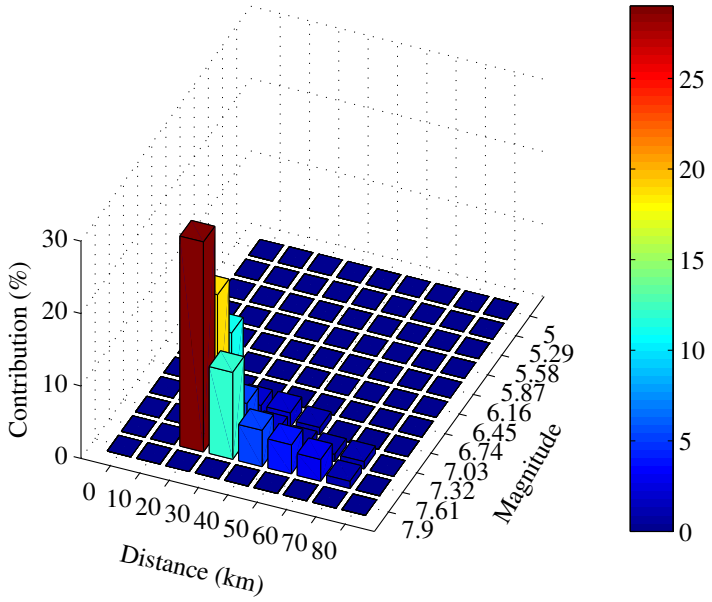

Figure 2.21. Deaggregation results for SA(T=4s), 475 years return period (Model 2 – BA2008).

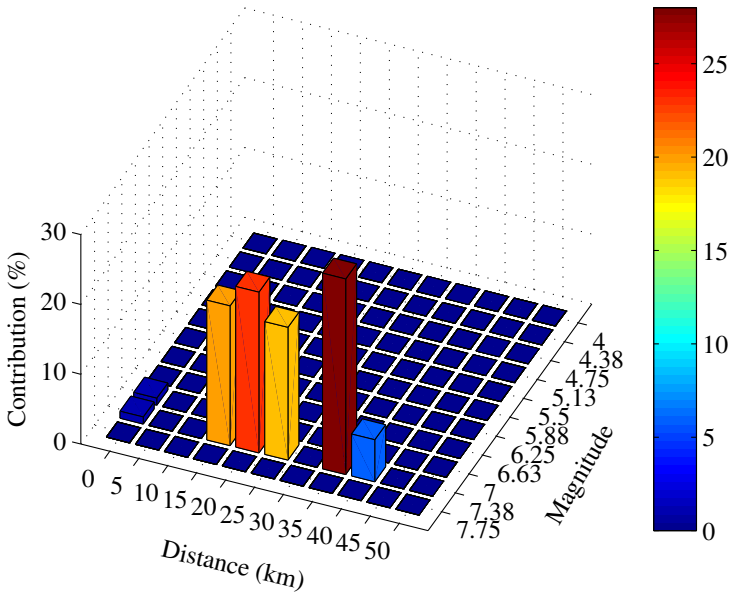

Figure 2.22. Deaggregation results for SA(T=4s), 475 years return period (Model 1 – CB2008).

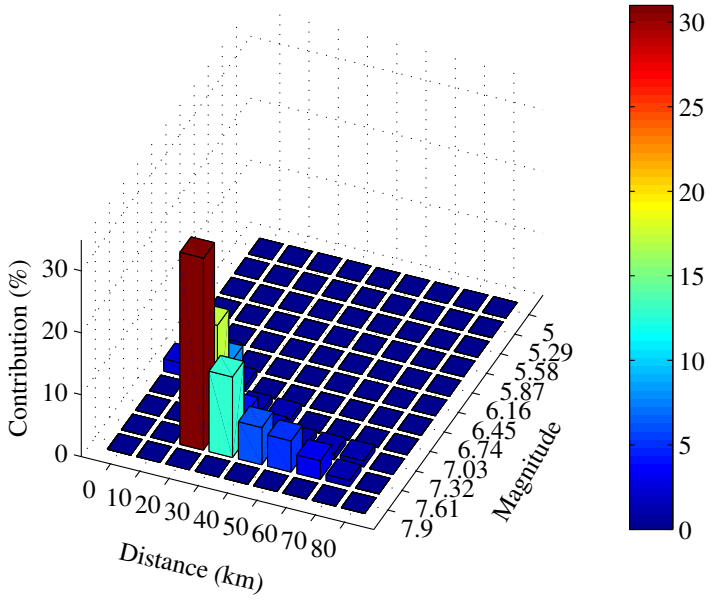

Figure 2.23. Deaggregation results for SA(T=4s), 475 years return period (Model 2 – CB2008).

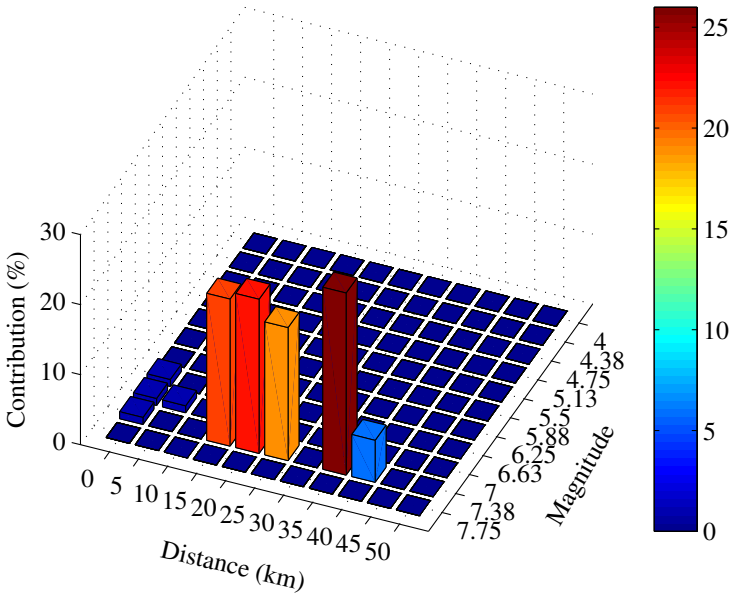

Figure 2.24. Deaggregation results for SA(T=4s), 475 years return period (Model 1 – CY2008).

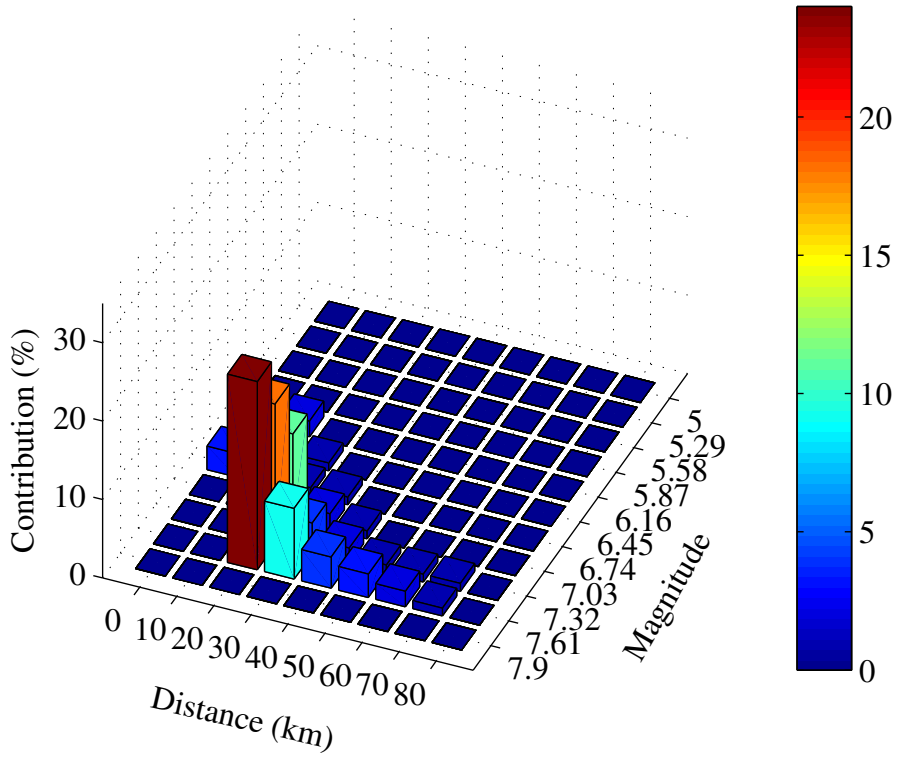

Figure 2.25. Deaggregation results for SA(T=4s), 475 years return period (Model 2 – CY2008).

2.5. Ground Motion Record Selection

Selection of the ground motion records is done with the help of *Peer Strong Motion Database NGA-West 2 Ground Motion Selection Tool*. Seven input ground motion records are selected for each model and each GMPE (i.e. for each sub-model). In other words 42 records are selected (2x3x7=42) and scaled in total to be used in linear time-history analyses of a finite element model. Seven input records for a sub-model are selected in accordance with the deaggregation result for corresponding sub-model. Number of ground motion records for each magnitude-distance pair is determined according to contributions of each magnitude-distance pair. Figure 2.26 in accordance with Table 2.10 clarifies this procedure for one of the sub-models.

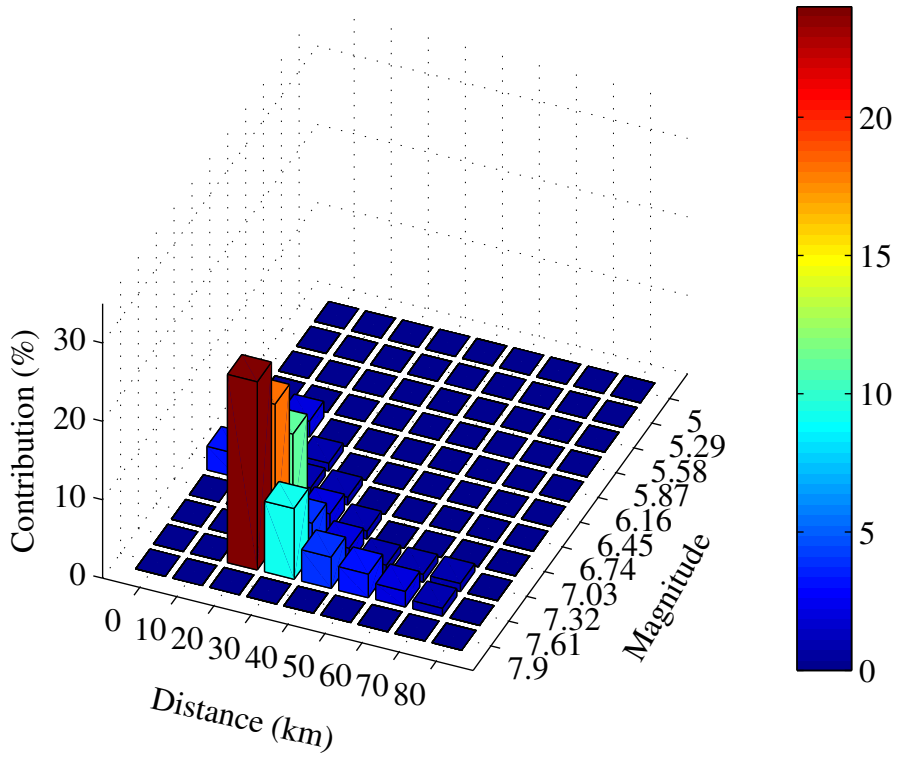

Figure 2.26. Deaggregation results for Model 2 – CY2008 for ground motion record selection.

Table 2.10. Magnitude – distance ranges of selected records according to deaggregation results for Model 2 – CY2008.

Number of records selected	**Distance interval (km)**	**Magnitude interval**
3	15 - 25	7.45 - 7.75
2	15 - 25	7.15 - 7.45
1	15 - 25	6.75 - 7.15
1	25 - 35	7.45 - 7.75

Records are selected in a way that, geometric mean of the scaled response spectra of earthquakes is compatible with 1.3 times the UHS of corresponding sub-model. According to ASCE 7-05, geometric mean of the response spectra of selected earthquakes should not be below 1.3 times the target UHS between $0.2T_1$ and $1.5T_1$, where T_1 is the fundamental period of the structure. The idea behind this is considering the higher mode effects (by $0.2T_1$) which can be significant for tall structures, and considering the period elongation due to yielding of structural components (by $1.5T_1$). Response spectrum of each earthquake is actually square root of the sum of the squares (SRSS) of the response spectra of the record in two horizontal directions.

Scaling of the earthquake records are done by minimizing the mean square error (MSE) method. Minimizing MSE aims to minimize the difference between scaled mean response spectrum and the target UHS at the desired periods specified by user. There is another scaling method which is called conditional mean spectrum (Baker, 2011). This method aims to have a perfect match between mean response spectra and target UHS at only a single period.

Time-history of each component of each scaled-earthquake record is checked for their significant durations. In most of the seismic design codes (i.e. TSC 2007), it is suggested that duration between the first and last points above 0.05g accelerations should not be less than 15 seconds or five times the fundamental period of the structure.

SRSS of response spectra of seven selected earthquakes in two-directions, geometric mean spectrum and 1.3 times the target UHS, for each sub-model is given in Figures 2.27 to Figure 2.32 All the details of the earthquake records are also given in the tables below each figure for each sub-model.

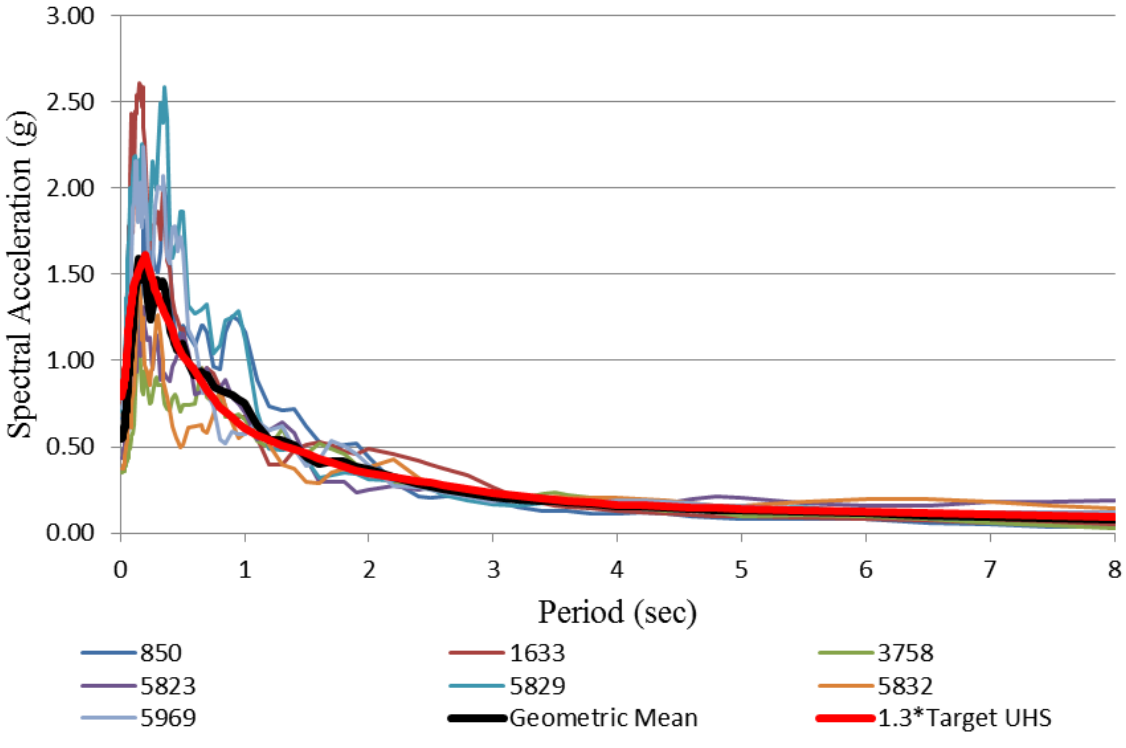

Figure 2.27. Target UHS vs response spectra of selected earthquake records and mean of their response spectra for Model 1-BA2008.

Table 2.11. Information about selected and scaled ground motion records for Model 1-BA2008.

ID	Earthquake	Station	Year	Mech.	M	SF	Rrup
850	Landers	Desert Hot Springs	1992	SS	7.28	2.83	21.78
1633	Manjil	Abbar	1990	SS	7.37	1.03	12.55
3758	Landers	Thousand Palms Post Office	1992	SS	7.28	2.30	36.93
5823	El Mayor-Cucapah	Chihuahua	2010	SS	7.20	1.37	19.47
5829	El Mayor-Cucapah	RIITO	2010	SS	7.20	1.28	13.71
5832	El Mayor-Cucapah	TAMAULIPAS	2010	SS	7.20	1.22	26.55
5969	El Mayor-Cucapah	Bonds Corner	2010	SS	7.20	2.16	32.85

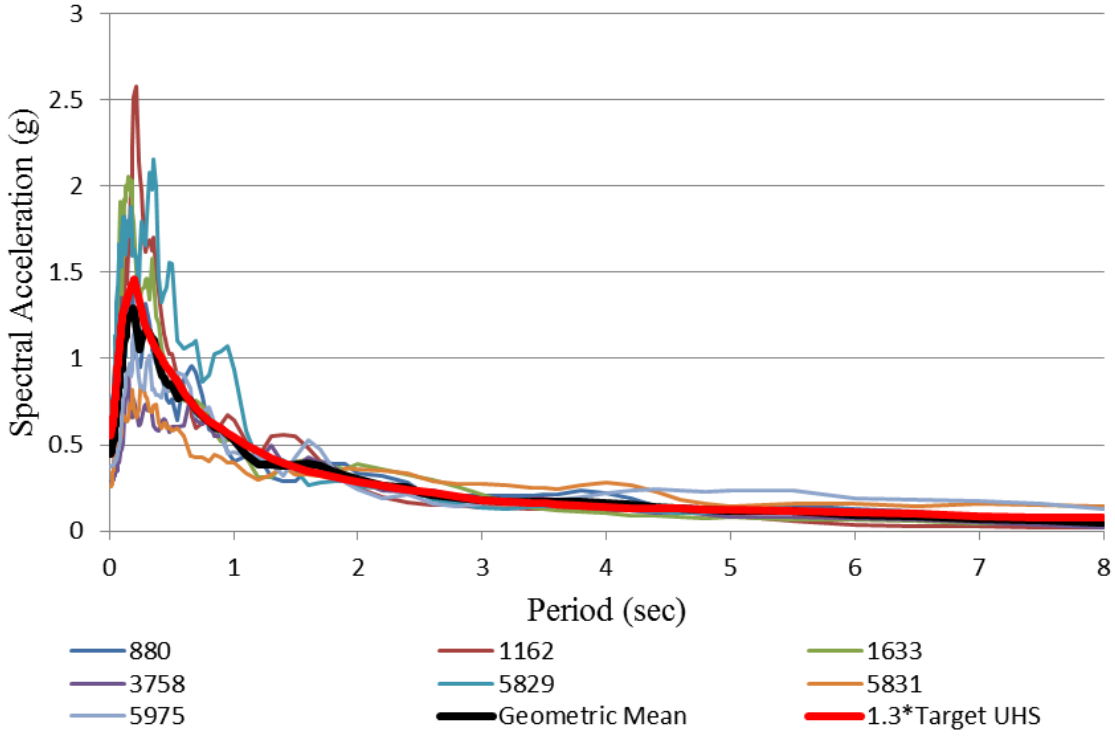

Figure 2.28. Target UHS vs response spectra of selected earthquake records and mean of their response spectra for Model 1-CB2008.

Table 2.12. Information about selected and scaled ground motion records for Model 1-CB2008.

ID	Earthquake	Station	Year	Mech.	M	SF	Rrup
880	Landers	Mission Creek Fault	1992	SS	7.28	3.17	26.96
1162	Kocaeli	Goynuk	1999	SS	7.51	3.41	31.74
1633	Manjil	Abbar	1990	SS	7.37	0.82	12.55
3758	Landers	Thousand Palms Post Office	1992	SS	7.28	1.87	36.93
5829	El Mayor-Cucapah	RIITO	2010	SS	7.20	1.06	13.71
5831	El Mayor-Cucapah	EJIDO SALTILLO	2010	SS	7.20	1.23	17.32
5975	El Mayor-Cucapah	Calexico Fire Station	2010	SS	7.20	1.00	20.46

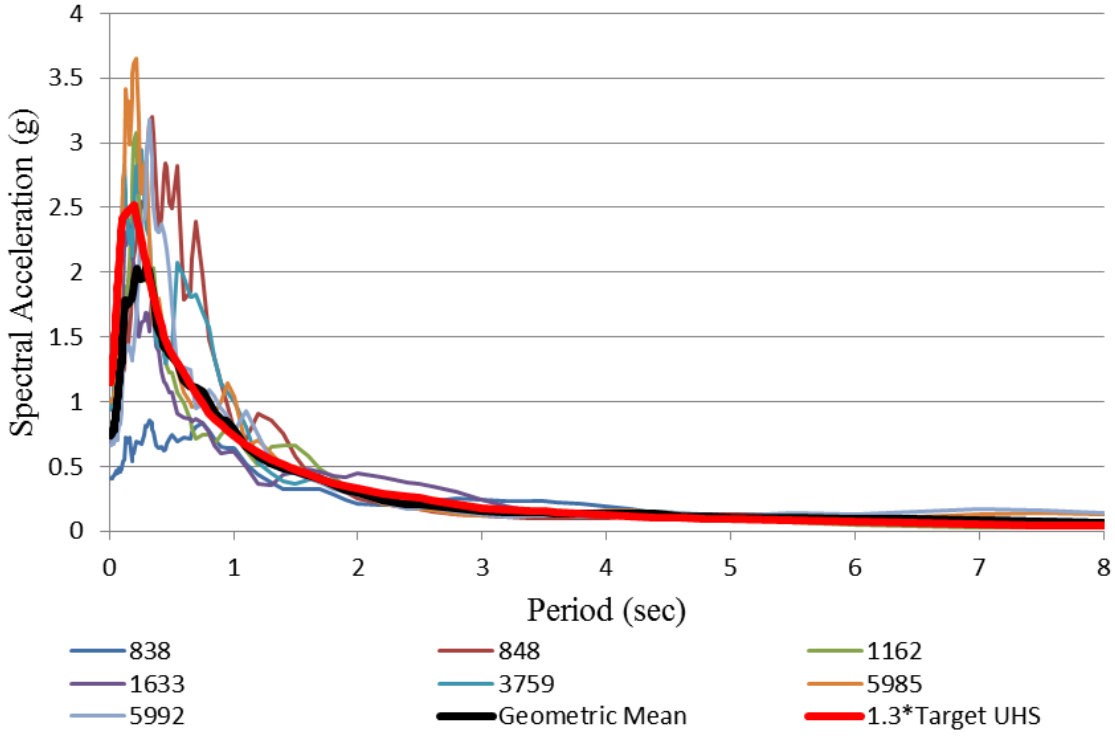

Figure 2.29. Target UHS vs response spectra of selected earthquake records and mean of their response spectra for Model 1-CY2008.

Table 2.13. Information about selected and scaled ground motion records for Model 1-CY2008.

ID	Earthquake	Station	Year	Mech.	M	SF	Rrup
838	Landers	Barstow	1992	SS	7.28	2.17	34.86
848	Landers	Coolwater	1992	SS	7.28	1.86	19.74
1162	Kocaeli	Goynuk	1999	SS	7.51	4.07	31.74
1633	Manjil	Abbar	1990	SS	7.37	0.94	12.55
3759	Landers	Whitewater Trout Farm	1992	SS	7.28	5.38	27.05
5985	El Mayor-Cucapah	El Centro Differential Array	2010	SS	7.20	1.33	23.42
5992	El Mayor-Cucapah	El Centro Array 11	2010	SS	7.20	0.90	16.21

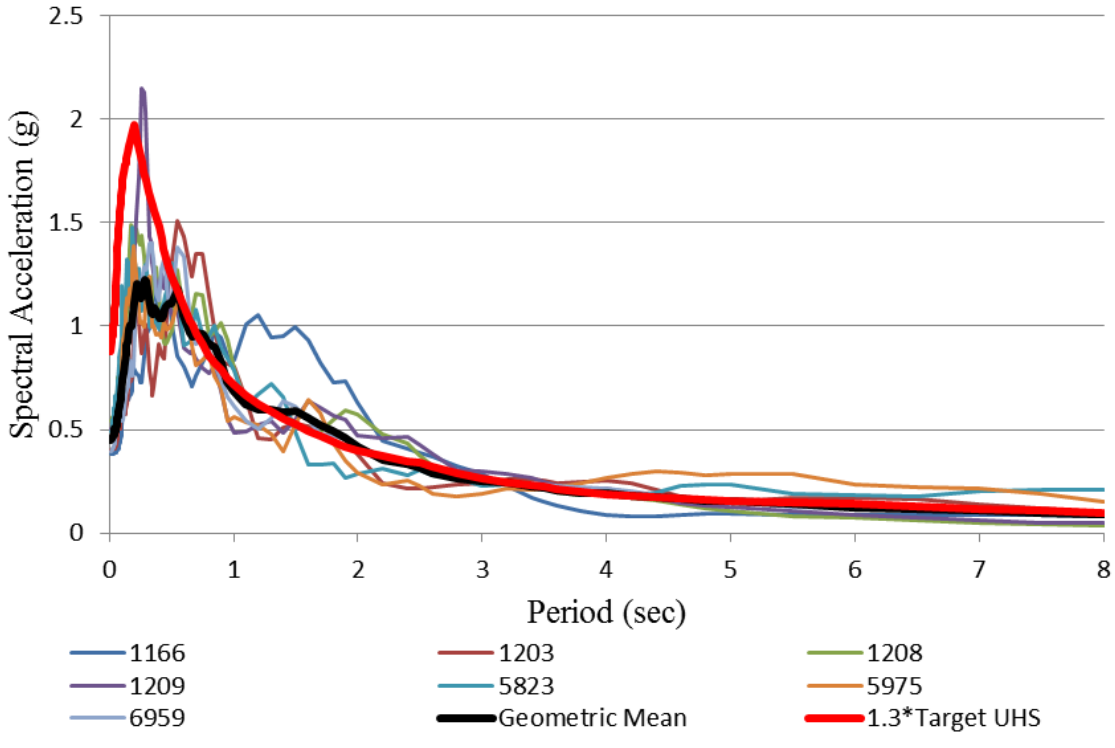

Figure 2.30. Target UHS vs response spectra of selected earthquake records and mean of their response spectra for Model 2-BA2008.

Table 2.14. Information about selected and scaled ground motion records for Model 2-BA2008.

ID	Earthquake	Station	Year	Mech.	M	SF	Rrup
1166	Kocaeli	Iznik	1999	SS	7.51	2.48	30.73
1203	Chi-Chi	CHY036	1999	RO	7.62	1.18	16.04
1208	Chi-Chi	CHY046	1999	RO	7.62	2.25	24.10
1209	Chi-Chi	CHY047	1999	RO	7.62	2.05	24.13
5823	El Mayor-Cucapah	Chihuahua	2010	SS	7.20	1.54	19.47
5975	El Mayor-Cucapah	Calexico Fire Station	2010	SS	7.20	1.21	20.46
6959	Darfield	Christchurch Resthaven	2010	SS	7.00	1.12	19.48

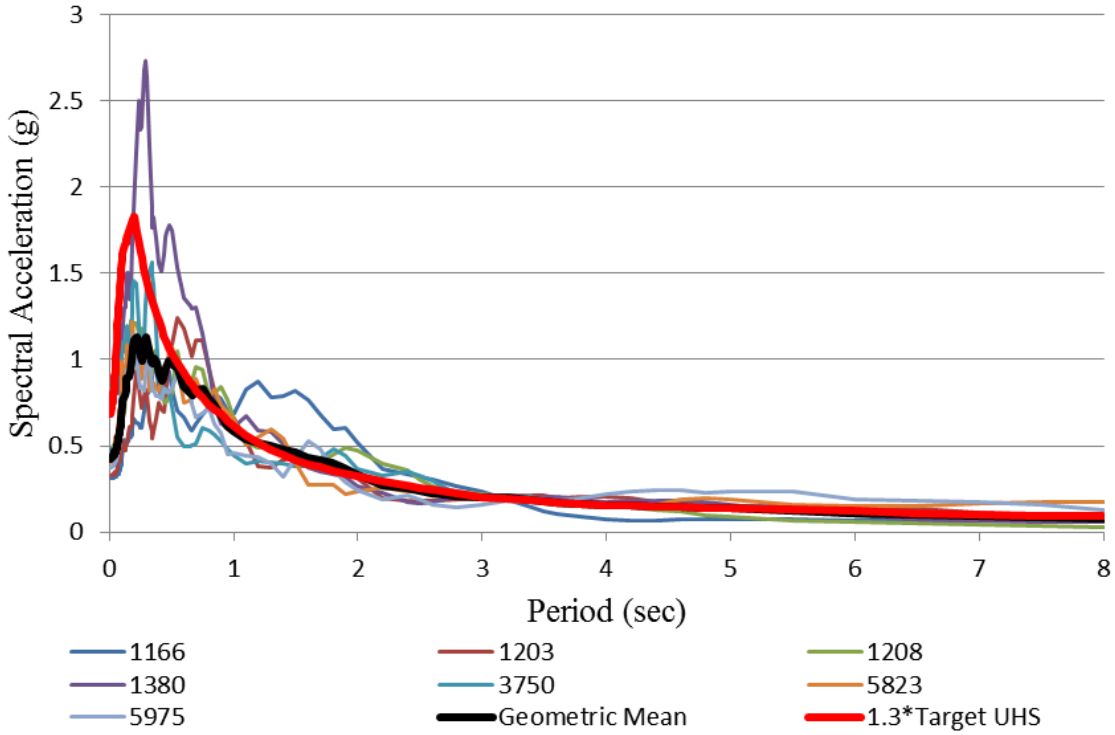

Figure 2.31. Target UHS vs response spectra of selected earthquake records and mean of their response spectra for Model 2-CB2008.

Table 2.15. Information about selected and scaled ground motion records for Model 2-CB2008.

ID	Earthquake	Station	Year	Mech.	M	SF	Rrup
1166	Kocaeli	Iznik	1999	SS	7.51	2.05	30.73
1203	Chi-Chi	CHY036	1999	RO	7.62	0.97	16.04
1208	Chi-Chi	CHY046	1999	RO	7.62	1.85	24.10
1380	Chi-Chi	KAU054	1999	RO	7.62	6.59	30.85
3750	Cape Mendocino	Loleta Fire Station	1992	R	7.01	1.29	25.91
5823	El Mayor-Cucapah	Chihuahua	2010	SS	7.20	1.27	19.47
5975	El Mayor-Cucapah	Calexico Fire Station	2010	SS	7.20	1.00	20.46

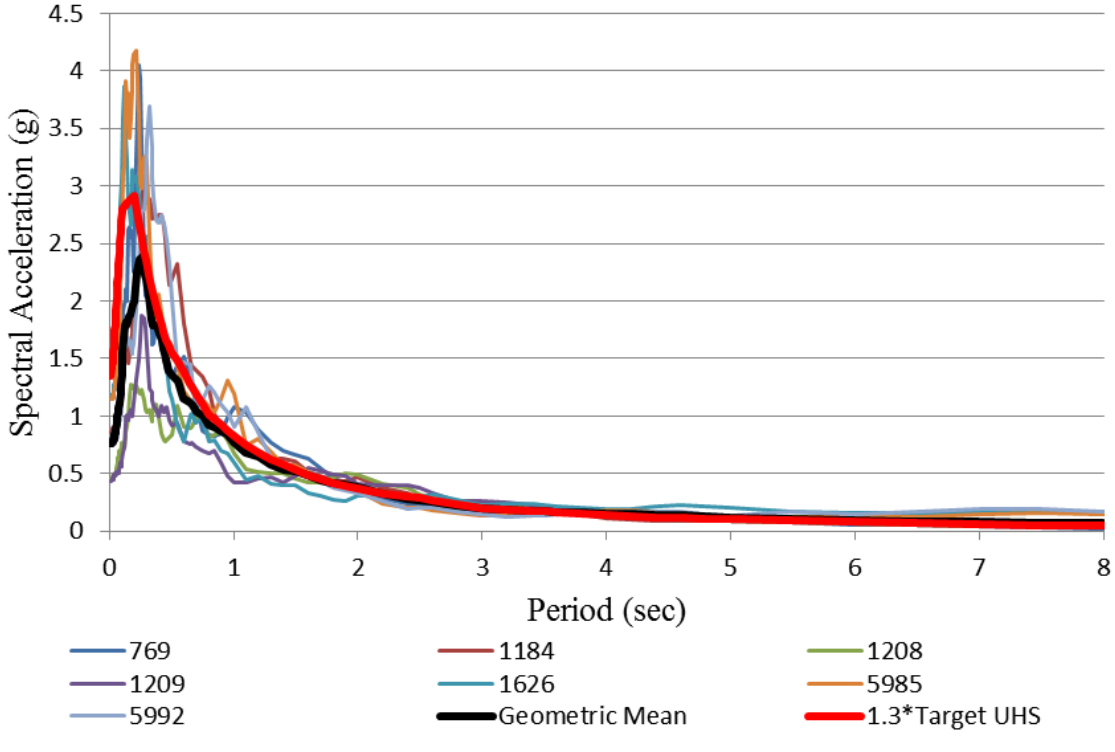

Figure 2.32. Target UHS vs response spectra of selected earthquake records and mean of their response spectra for Model 2-CY2008.

Table 2.16. Information about selected and scaled ground motion records for Model 2-CY2008.

ID	Earthquake	Station	Year	Mech.	M	SF	Rrup
769	Loma Prieta	Gilroy Array 6	1989	RO	6.93	3.76	18.33
1184	Chi-Chi	CHY010	1999	RO	7.62	3.04	19.96
1208	Chi-Chi	CHY046	1999	RO	7.62	1.93	24.10
1209	Chi-Chi	CHY047	1999	RO	7.62	1.78	24.13
1626	Sitka-Alaska	Sitka Observatory	1972	SS	7.68	8.71	34.61
5985	El Mayor-Cucapah	El Centro Differential Array	2010	SS	7.20	1.52	23.42
5992	El Mayor-Cucapah	El Centro Array 11	2010	SS	7.20	1.05	16.21

3. THE STRUCTURE

3.1. General Information

Linear time-history analyses are conducted with 42 different earthquake records with a finite element model of a real reinforced-concrete tall structure. Structure is located in business center of Istanbul. Most of the high-rise buildings in Istanbul are also located in this area. The closest distance between the structure and the NAF is about 25km. Faults and the location of the building are shown in Figures 3.1 and 3.2.

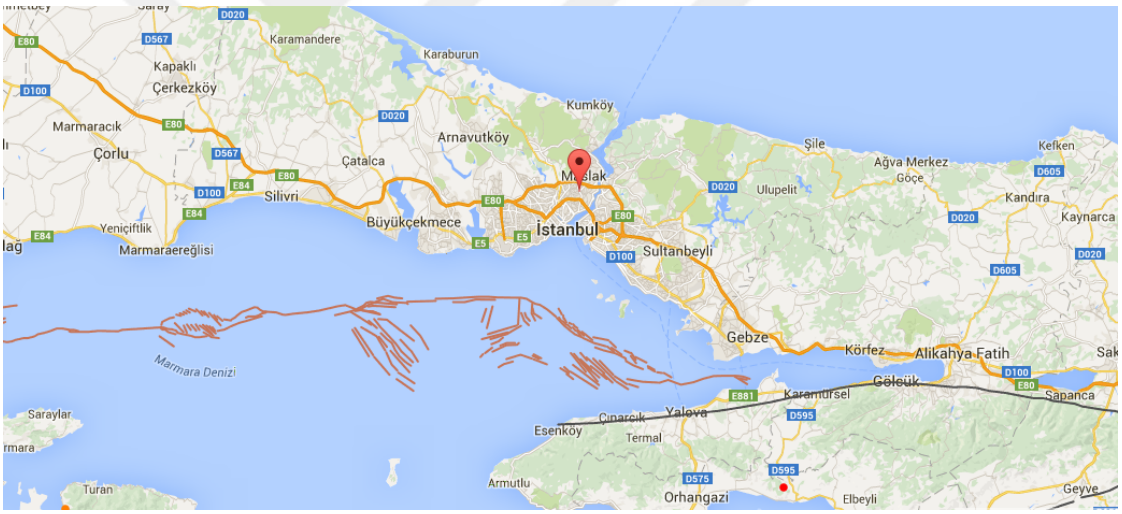

Figure 3.1. Position of the structure and faults.

Structure consists of tower section and the podium part. Most of the structure is used as office. Tower section and the podium part are separated with dilatation. In this study, only the tower part is modeled and analyzed.

Structure has a 166m height with 43 storys above ground level. Below ground level there are seven storys with 24m depth in total. A typical story at the tower section has a 1300 square meter area and 3.9m height. The general view of the structure is

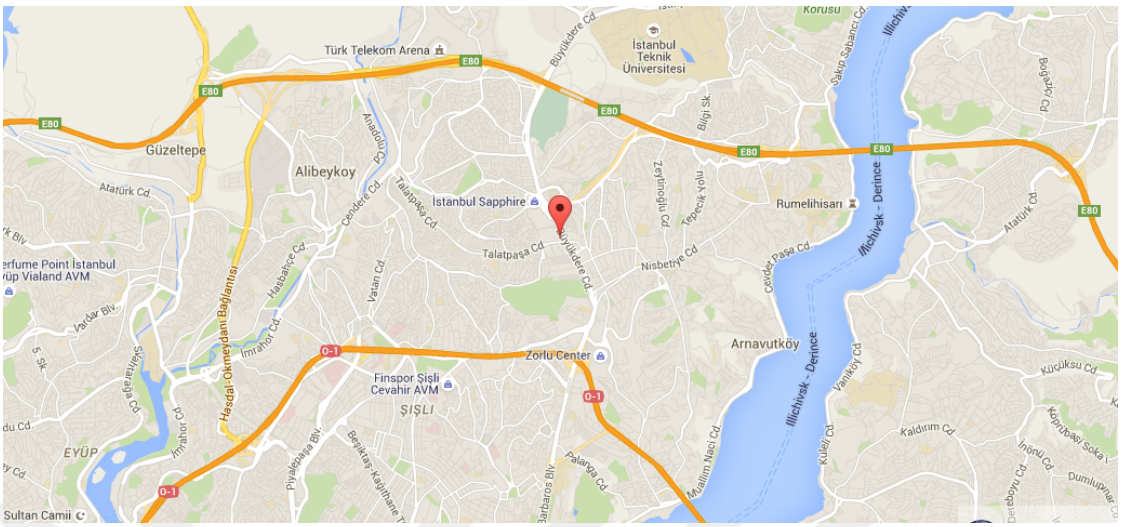

Figure 3.2. Position of the structure.

given in Figure 3.3. Typical tower story consists of peripheral columns connected with beams, two core walls which are connected to each other with deep steel beams, and flat slab (Figure 3.4). Typical floor has a 38m by 34m dimensions in X and Y directions, respectively. Peripheral columns are placed such that, tower has a parallelogram shape. Columns are connected to core wall via slab only. Slabs in typical storys were adjusted such that, slabs at sharp corners of structure have 260mm thickness (due to longer clearspan), whereas other parts have 220mm. Columns at the lower storys of the tower have composite section. I-section steel columns are embedded into 1m diameter circular reinforced concrete columns as seen in Figure 3.5. Thickness of the structural wall starts with 700mm at the bottom and decreases to 500mm at top storys. Materials used in construction of the structure are summarized in Table 3.1.

As seen in Figure 3.7 and Figure 4.2, there are mezzanines at 8th, 9th, 18th, 19th, 28th and 29th story of structure. Those storys do not have a reinforced concrete slab as other floors, but they have thinner composite slabs (Figure 3.6). Two mezzanine floors are hanged with steel sections to the upper floor which is thicker than the other typical story slabs (400mm), and mezzanines are also supported with anchorages to the core wall and columns. At the entrance level, story height is about 9m, this is also visible in Figure 3.7 and Figure 4.2.

Table 3.1. Material properties used in construction.

	Material class	**Young's Modulus (MPa)**
Foundation	C40	34000
Peripheral beams, columns and structural walls	C45	36000
Reinforcement bars	S420	210000
Steel beam connecting cores each other	St44	210000
Steel sections embedded in compoesite columns	St52	210000
Mezzanine composite deck	St37	210000

Figure 3.3. General view of the structure.

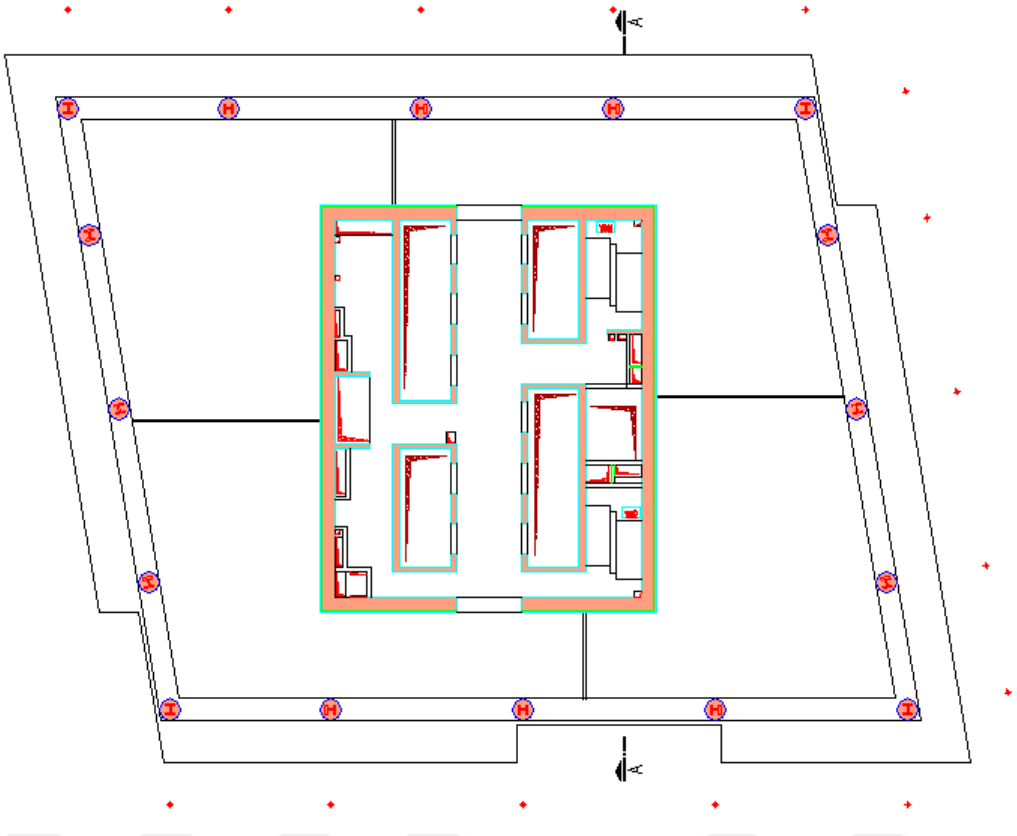

Figure 3.4. Plan drawing of a typical story.

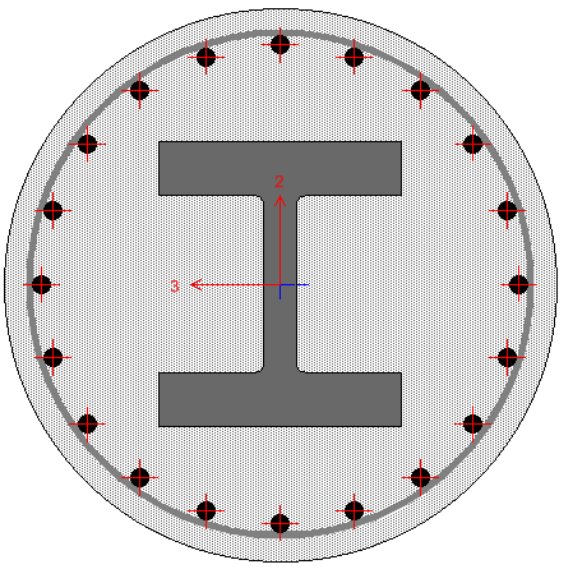

Figure 3.5. Cross section of a composite column.

Figure 3.6. Plan drawing of a mezzanine story.

3.2. Finite Element Model

Linear finite element model (FEM) of the tower section is constructed with ETABS software with the help of design drawings. Frame elements are used for columns and beams, whereas shell elements are used for shear walls and slabs. Model is constructed as detailed as possible. Mezzanines are also modeled according to design drawings again. Since there are no beams between the columns and the core wall and slabs are already modeled with shell elements, diaphragms are avoided to use in model. Lateral springs are used in order to represent the effect of soil around the structural walls below ground level. Spring coefficients for these lateral springs are taken from design report of the structure. Foundation of the structure is assumed to be fixed in structural model, therefore not modeled as a slab. Damping ratio of the structure is assumed to be 1.5% according to design report. Extruded 3-D view of the FEM is given in Figure 3.7.

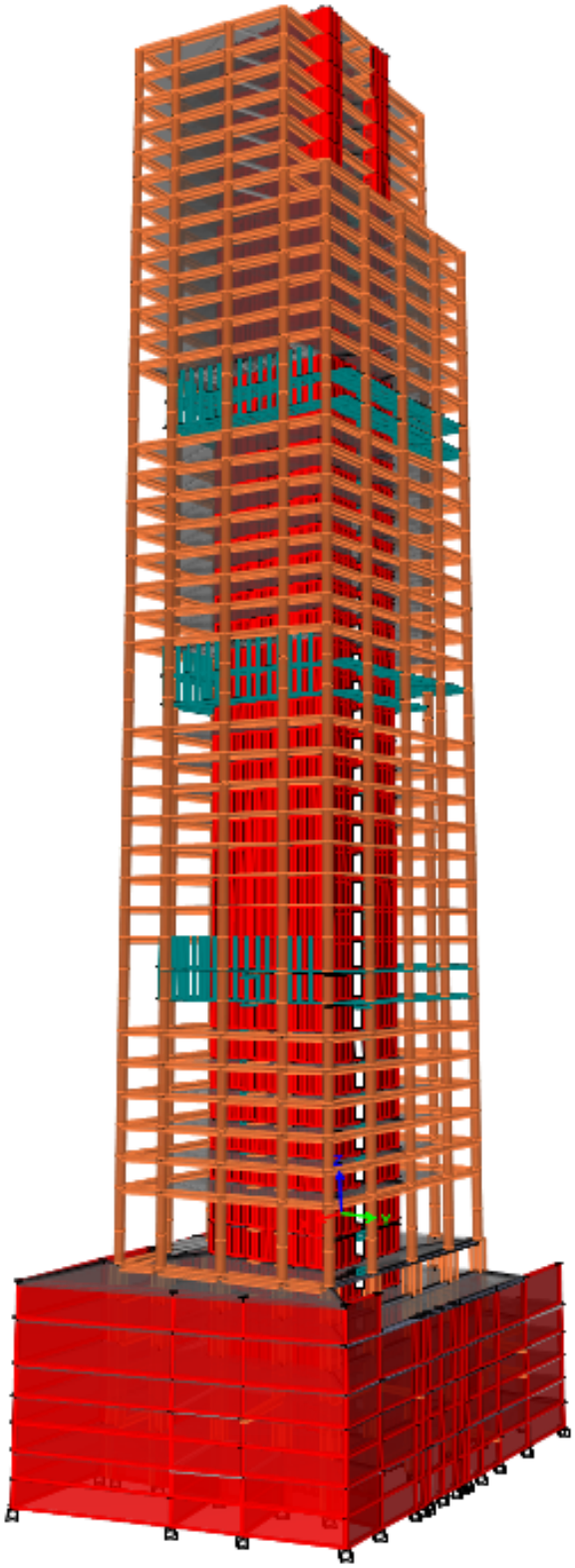

Figure 3.7. Finite element model of the structure.

Loads and material properties are directly taken from the design report of the structure. Material properties used in modeling were given in Table 3.1 in General Information section and the gravity loads applied to the structure is given in Table 3.2.

Table 3.2. Gravity loads considered in structural model.

Dead loads	Typical floors	2.0kN/m^2
	Roof	5.0kN/m^2
	Ground level and below	3.1kN/m^2
Live loads	Office and residence	2.0kN/m^2
	Corridors	3.5kN/m^2
	Mechanic areas	7.5kN/m^2
Façade (Dead load)	Peripheral beams	1.2kN/m^2

Modal analysis is conducted and the first three mode shapes are presented in Figure 3.8 and mode frequencies are given in Table 3.3. Mode frequencies are usually identified higher when the system identification is done with ambient measurements compared to measurements taken during an earthquake. This phenomenon is observed in many research (Skolnik *et al.*, 2006). In addition to this, since structure did not experienced any significant ground motion and the validation of FEM is done according to system identification results obtained from ambient measurements, un-cracked section properties are used in modal analysis.

Table 3.3. Summary of mode frequencies.

	X1	**X2**	**X3**	**Y1**	**Y2**	**Y3**	**T1**	**T2**
T(sec)	4.170	1.070	0.508	3.298	0.663	0.279	1.652	0.549
f(1/sec)	0.240	0.935	1.968	0.303	1.508	3.584	0.605	1.812

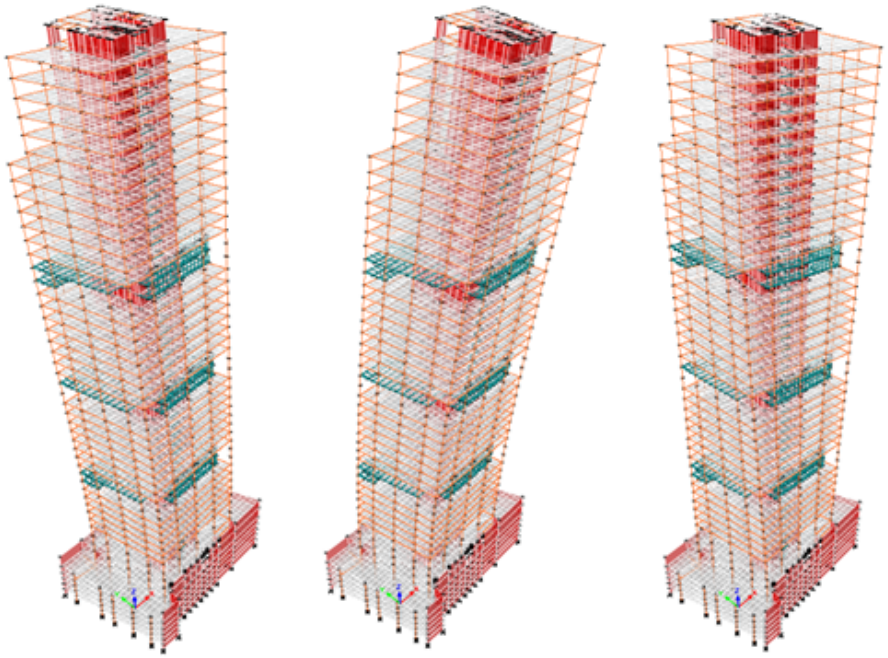

Figure 3.8. Mode shapes of structural model.

Non-linear FEM of the structure was also constructed. All structural elements including structural walls (except slabs) of the structure modeled with frame elements in nonlinear structural model in order to decrease the computational time of nonlinear time-history analysis. Fundamental translational mode shapes and frequencies of this model were similar to linear FEM; however, torsional mode frequency was approximately half of the linear FEM. Since the only difference of these models was modeling method of structural wall, this discrepancy is attributed to frame assumption of structural wall, but not proved. This discrepancy is also observed in Brownjohn *et al.*, (2000). Due to this unrealistic torsional behavior and long computational time, we decided to continue from linear FEM and revisit the nonlinear FEM in future studies.

A parametric study is conducted in order to observe the sensitivity of the FEM in terms of modal frequencies to the certain parameters and assumptions. These parameters and assumptions are Young's modulus of concrete, soil effect (by means of lateral restraints) and bending modifier of section (i.e. cracked or un-cracked EI values).

Reference model (Ec=36000MPa, soil spring coefficient k=75000kN/m and EI coefficient=1.00) is compared with other models in which only one parameter is changed while others kept constant (values of reference model). Modulus of elasticity of concrete can be estimated with relations which is different for different design codes. Modulus of elasticity value used in reference model, Ec=36000MPa, is average of TS500 (Equation 3.1) and Eurocode (EN1994)(Equation 3.2). The average of these relations is used because relation of those codes yields similar results (35801MPa and 36283MPa, respectively). Equation 3.3 which is taken from ACI 318, yields 31528MPa. Since difference is significant, mode frequencies are obtained for this value as well.

$$3250\sqrt{f_c} + 14000(MPa) \tag{3.1}$$

$$22\left(\frac{f_c + 8}{10}\right)^{0.3}(GPa) \tag{3.2}$$

$$4700\sqrt{f_c}(MPa) \tag{3.3}$$

Lateral restrains on structural walls below ground level are adjusted such that they are free as they are not surrounded by soil, and their joints are fixed in translational X or Y direction in their normal direction, in order to observe the effect of lateral restraints.

For bending modifier effect, EI coefficient is adjusted to 0.40EI for all columns and beams and 0.70EI for structural walls (according to approximate gravity load on them) for EI Case 1, and for other case EI coefficient of slabs are changed to 0.25EI in addition to others as suggested in ACI 318 (EI Case 2).

All of the mode frequencies are noted and summarized in Table 3.4. According to Table 3.4 mode frequencies are not that sensitive to lateral restraints. This may be

due to the large structural walls below ground level which already increases the story stiffness significantly. Effect of Young's modulus is significant; therefore, uncertainty in estimating Young's modulus of concrete should be taken into account in structural modeling. Effect of bending modifiers are also very significant, however mode frequencies are very sensitive to the bending modifier used in slab elements more than other elements' bending modifiers. Reference model's values are used for our final model because, Young's modulus estimation is close to each other for two of three relations, the soil spring coefficient is already given as 75000kN/m in design report of structure and the mode frequencies are closest to identified ones as described in Chapter 4 with un-cracked section properties.

Table 3.4. Parametric study on some parameters and assumptions.

	Reference	**E_c=31528MPa**	**laterally free**	**laterally fixed**	**EI Case 1**	**EI Case 2**
f of mode X1	0.240/s	0.226/s	0.236/s	0.242/s	0.232/s	0.207/s
f of mode Y1	0.303/s	0.284/s	0.291/s	0.310/s	0.297/s	0.280/s

4. SYSTEM IDENTIFICATION

4.1. Instrumentation

System identification (SID) process is applied for validation of the FEM. For this purpose, 11 acceleration sensors and a dynamic data acquisition system is instrumented on building (Figure 4.1). Data acquisition system is a 16 channel device which collects all data taken from accelerometers. As Figure 4.2 indicates, six stations are determined for sensors throughout the building. Stations are at -6th, entrance, 10th, 20th, 30th and 40th storys. Two sensors, in X and Y horizontal directions, are placed at each station, except entrance and 40th floor stations. To be able to observe torsional behavior of the tower, one extra sensor at 40th story will be placed at the corner of the story. Due to practical reasons placement of that extra sensor is postponed. Since we had 11 acceleration sensors available, entrance floor (which is considered to be less important than other storys due to small modal displacements at mode shapes) is passed without sensors. Typical sensors are placed on main shear wall in order to observe the buildings global behavior, not a local behavior.

Figure 4.1. Data acquisition system, sensors and instrumented sensors.

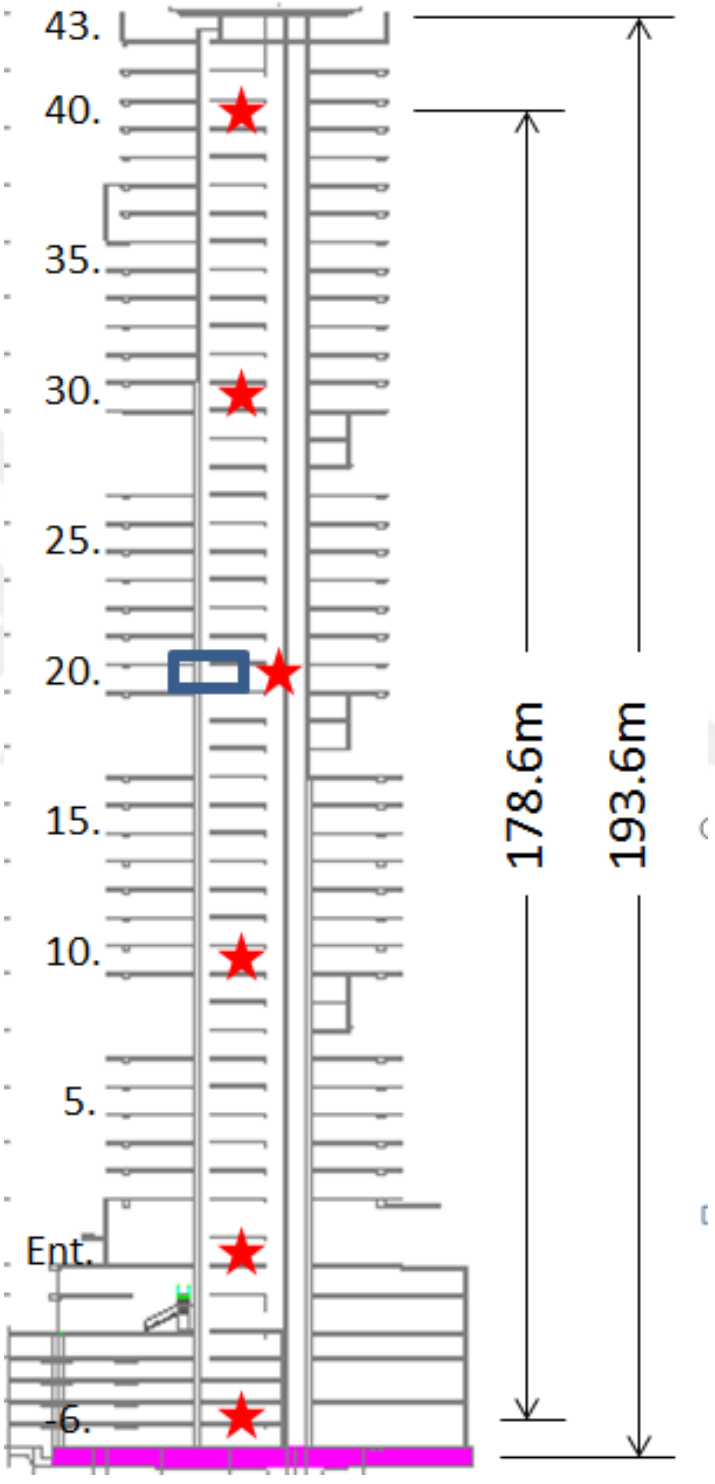

Figure 4.2. Location of data acquisition system, sensors and instrumented sensors.

Six more sensors will be placed on the structure. One of them will be the extra sensor at top, in order to observe torsional behavior of the structure, two of them will be at the entrance station in X and Y directions, and the rest will be placed at the -6th story station in vertical direction in order to investigate the rocking effect.

4.2. System Identification of The Structure

Dynamic properties of a structure can be estimated with the help of mathematical models. These models are generally considered to represent the actual dynamic behavior of the structure. This assumption may hold sometimes but usually it does not. Approximations done during the modeling and the limited knowledge about the real behavior of all structural elements may lead to errors in mathematical models. In order to verify the mathematical model or calibrate it to represent the real behavior, system identification methods can be employed. There are several system identification methods developed. Some of these methods need both input and the output measurements to identify the structure, whereas there are methods that do not need input data. Frequency domain decomposition (FDD) method is one of them, which is used in this thesis to identify the dynamic properties of the structure.

Frequency domain decomposition is a method which is presented in Brincker *et al.*, (2000). FDD is a useful tool when only the response measurements are available. By analyzing the response measurement dominating frequencies can be obtained. Therefore, even close modes can be detected by a fine discretization of frequency domain.

By using a MATLAB code written for FDD method, ambient vibration measurements taken from the structure are analyzed. Mode frequencies and mode shapes are extracted from analysis results and they are compared with mathematical model's results. Figure 4.3 shows the ambient vibration measurements taken from all stations in X direction, and Figure 4.4 and Figure 4.5 shows the mode frequencies observed after analyzing the data in X and Y directions, respectively. Peaks in Figure 4.4 and 4.5 with captions are translational mode frequencies. Since we could not place tor-

sional sensor on top, we can say that common peaks in both Figure 4.4 and Figure 4.5 without captions (0.528Hz, 1.593Hz and 2.734Hz) are probably the torsional mode frequencies. First two torsional mode frequencies are 0.605Hz and 1.812Hz according to FEM, which supports our prediction about identified torsional mode frequencies.

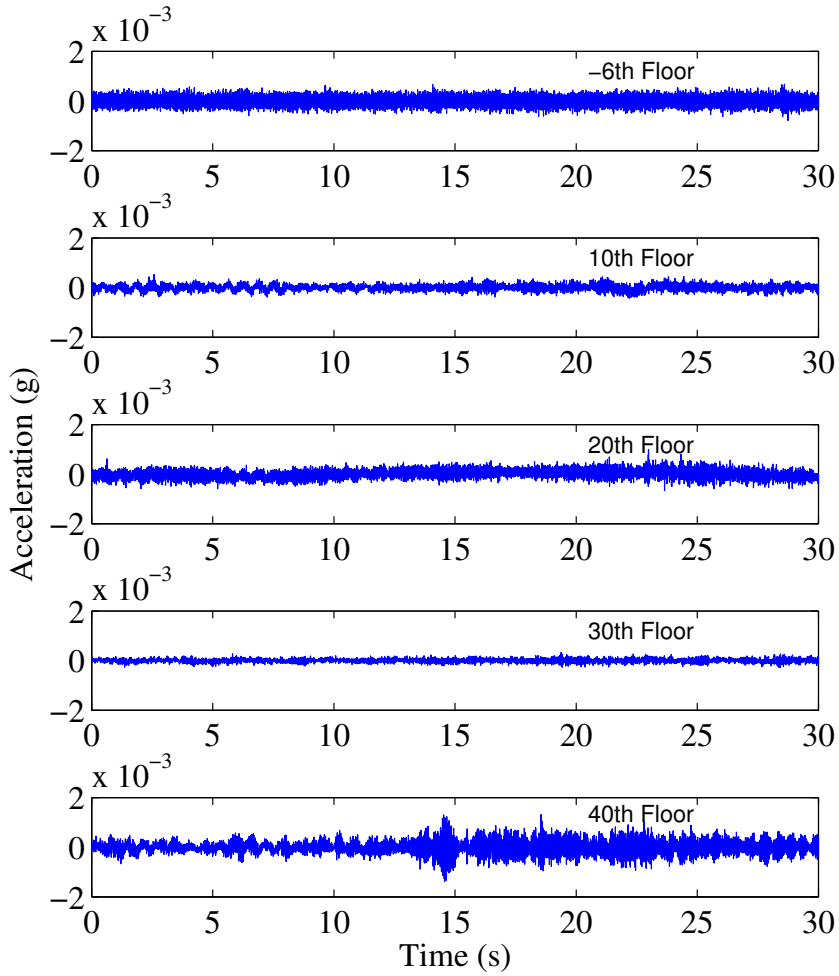

Figure 4.3. Sample data taken from acceleration sensors.

Mode shapes can also be obtained with the help of FDD method. Modal displacements for each dominating frequency in PSD graphs were extracted and mode shapes were plotted as seen in Figure 4.6. Mode frequencies and mode shapes obtained from SID and FEM are compared in Table 4.1 and Figure 4.7., respectively. Results

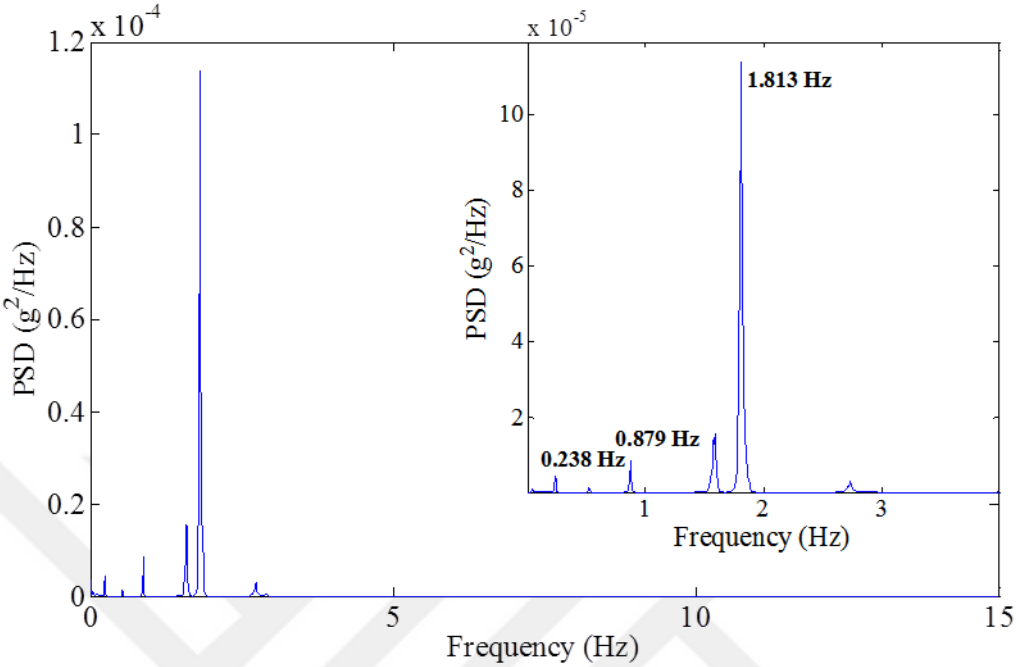

Figure 4.4. Analysis results of data in X direction.

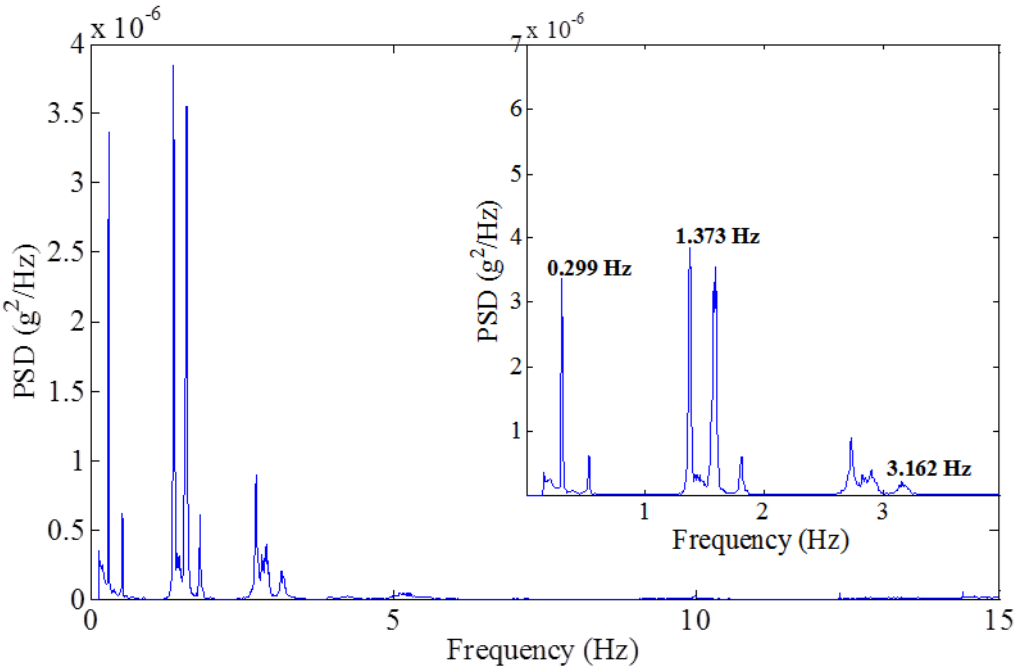

Figure 4.5. Analysis results of data in Y direction.

show that FEM represents almost the real behavior of the structure in terms of mode frequencies and mode shapes. FEM can be updated or calibrated by changing the uncertain parameters in the model. Since the differences are not that significant, with small adjustments on Young's Modulus of concrete or lateral soil spring coefficients within the range of uncertainty, better representation can be achieved. As mentioned above, differences can be neglected for our model, therefore, we continued with our FEM without any updating or calibration.

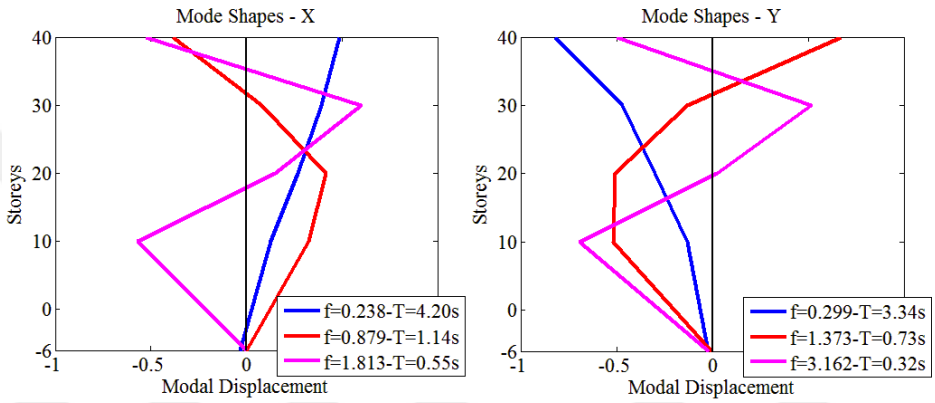

Figure 4.6. Mode shapes and frequencies obtained from FDD.

Table 4.1. Mode frequencies obtained from SID and FEM, and difference.

	Frequency from SID (1/sec)	**Frequency from FEM (1/sec)**	**Difference(%)**
X1	0.238/s	0.240/s	0.8
Y1	0.299/s	0.303/s	1.3
X2	0.879/s	0.935/s	6.4
Y2	1.373/s	1.508/s	9.8
X3	1.813/s	1.968/s	8.5
Y3	3.162/s	3.584/s	13.3

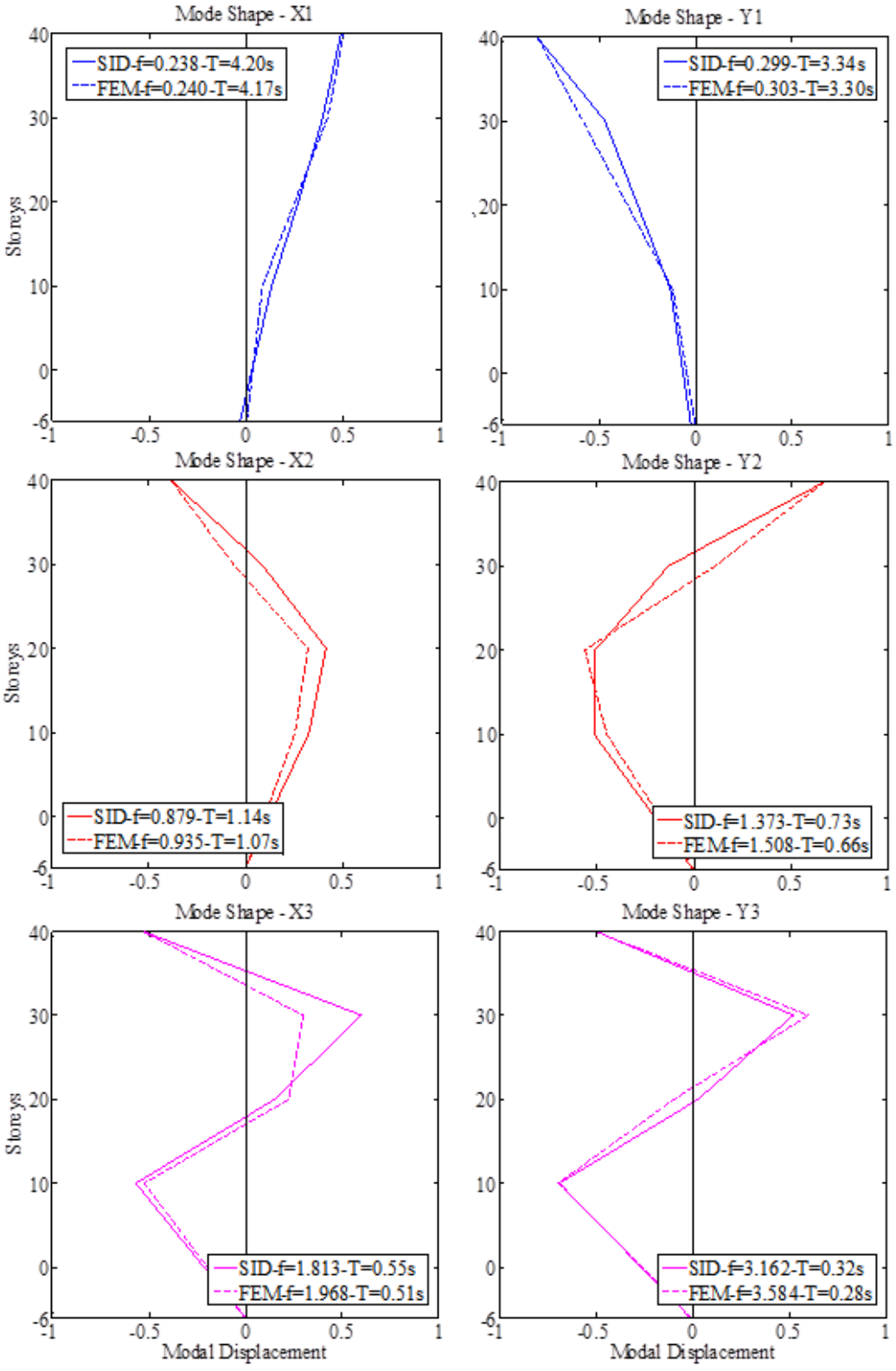

Figure 4.7. Mode shape and frequency comparison of SID and FEM results.

5. LINEAR TIME HISTORY ANALYSES

The main objective of this thesis is to investigate the effect of uncertainties in input ground motion selection on response of a tall structure. As mentioned before, inter-story drift ratios (IDR) are used as a response parameter. Linear time-time history analyses of a FEM are conducted for six sets of ground motion records with seven individual scaled input records (total of 42 records). Both of the horizontal components of earthquake records are applied to the FEM simultaneously in X and Y directions of building.

Inter-story drift ratios for each record, mean IDR and mean ±1 standard deviation IDR are given in figures below for both X and Y directions of the structure. IDR values exhibit kinks at certain elevations which are due to three mezzanine storey sections throughout the tower and the entrance level which has a 9m storey height. Kinks at IDR graphs are more clear in X direction with respect to Y direction. Since the X direction is weak direction of the structure this is expected. Up to a ground level IDR values are close to each other and are almost zero, which is due to large structural walls below ground level and soil pressure on them.

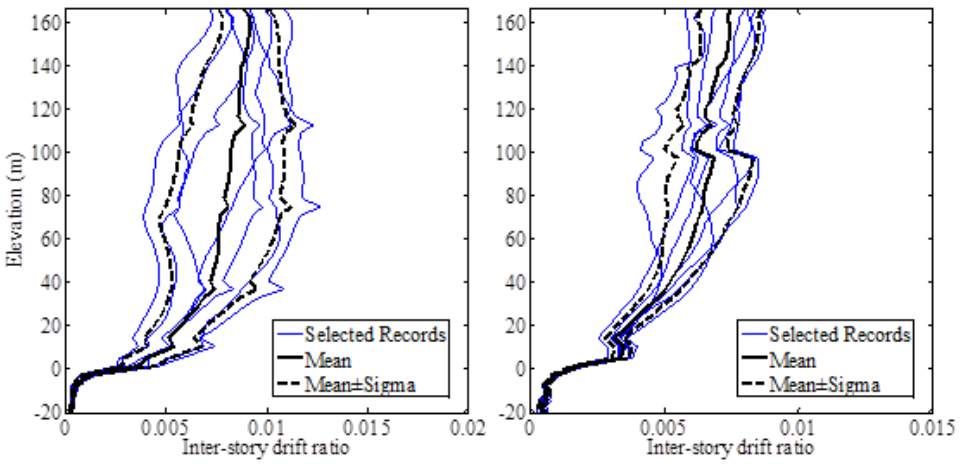

Figure 5.1. IDR, mean and mean ±1 standard deviation IDR in X and Y direction for Model 1 – BA2008 record set.

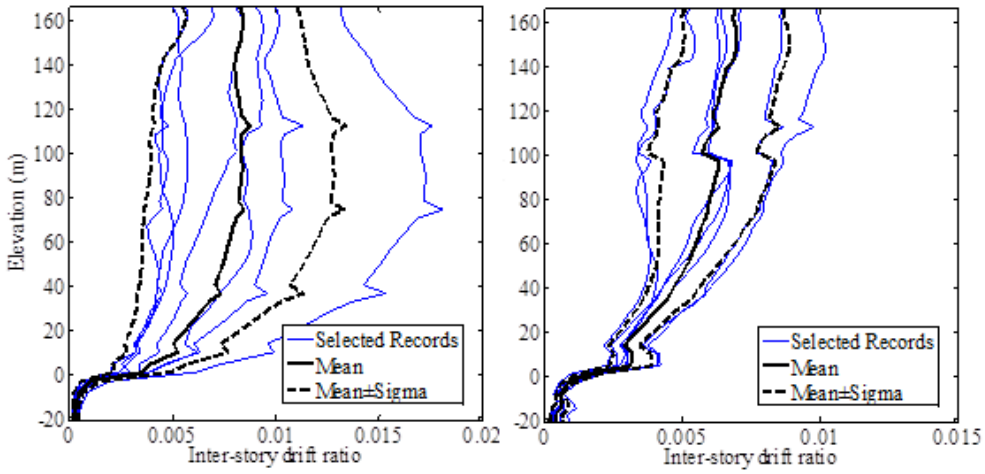

Figure 5.2. IDR, mean and mean ±1 standard deviation IDR in X and Y direction for Model 1 – CB2008 record set.

In order to compare effect of uncertainties in input selection easily, mean values of IDR are plotted on each other. Figure 5.7 compares GMPE selection effect when Model 1 is employed. Maximum difference between minimum and maximum mean IDR yielding sub-models along the height of tower, reaches up to 40% in both directions. For Model 2 same amount of difference is observed in Y direction, whereas in X direction maximum difference is about 26% (Figure 5.8).

When the effect of model selection (Model 1 or Model 2) is considered, maximum difference percentages are seems to depend on employed GMPE. When Model 1 is used with BA2008 maximum difference is about 32%, whereas for CB2008 and CY2008 maximum differences are 11% and 48%, respectively.

When all the sub-models are considered (Figure 5.12), maximum difference increases significantly up to 80% for each direction. All conclusions derived above are summarized in Table 5.1.

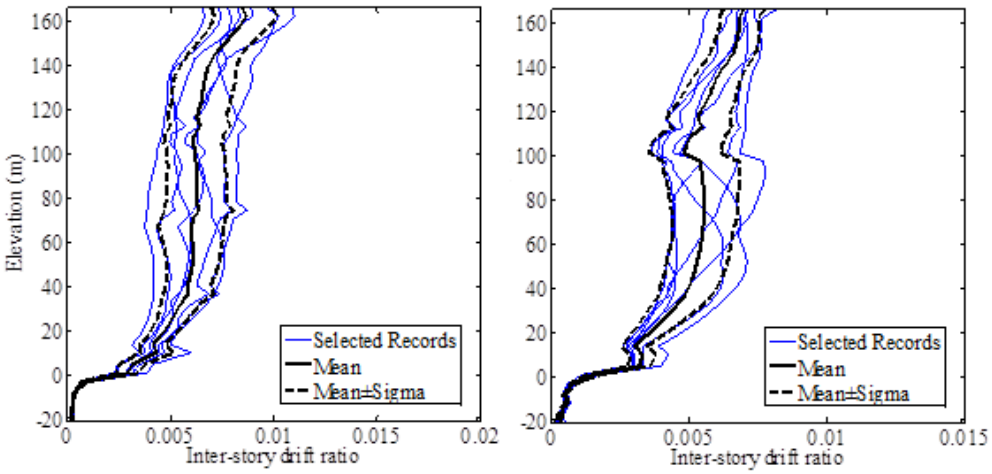

Figure 5.3. IDR, mean and mean ±1 standard deviation IDR in X and Y direction for Model 1 – CY2008 record set.

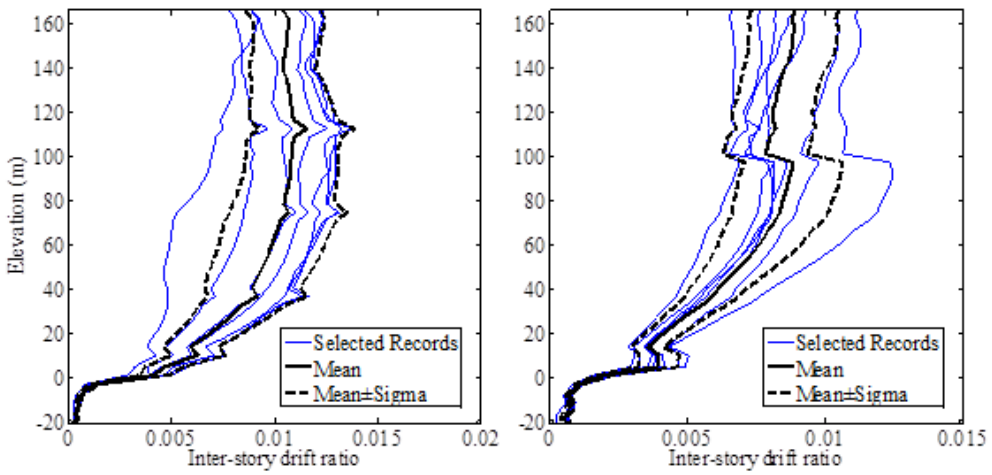

Figure 5.4. IDR, mean and mean ±1 standard deviation IDR in X and Y direction for Model 2 – BA2008 record set.

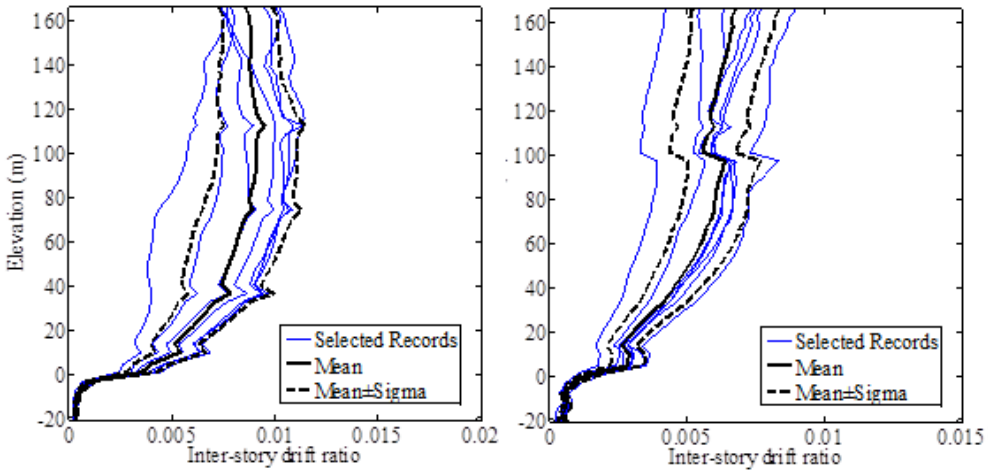

Figure 5.5. IDR, mean and mean ±1 standard deviation IDR in X and Y direction for Model 2 – CB2008 record set.

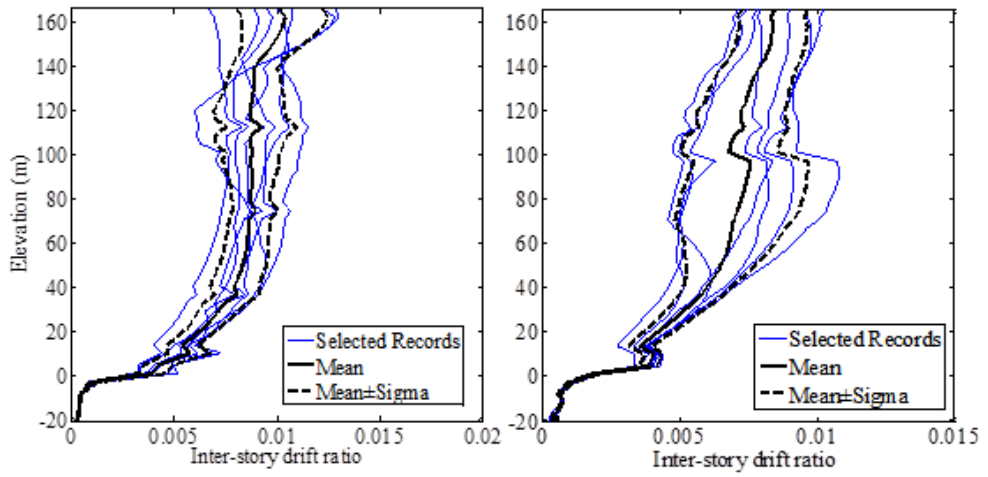

Figure 5.6. IDR, mean and mean ±1 standard deviation IDR in X and Y direction for Model 2 – CY2008 record set.

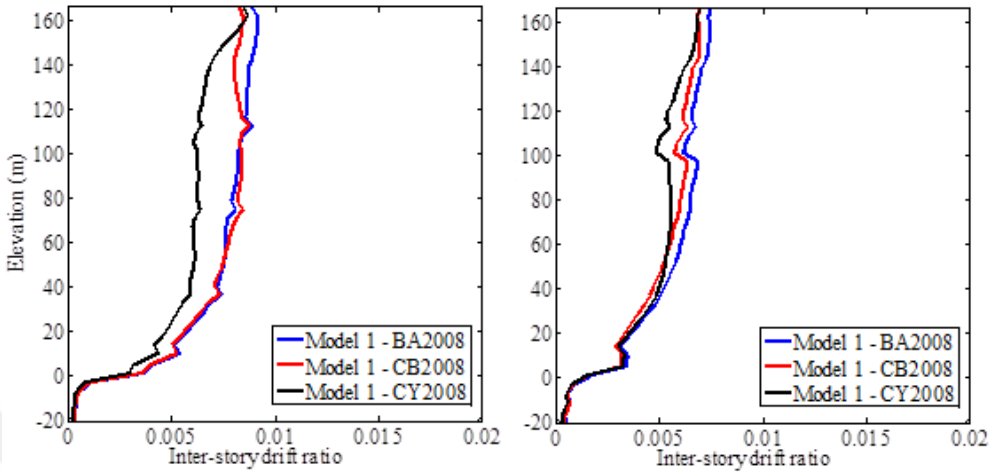

Figure 5.7. Mean IDR graphs for Model 1 with three different GMPEs in X and Y directions.

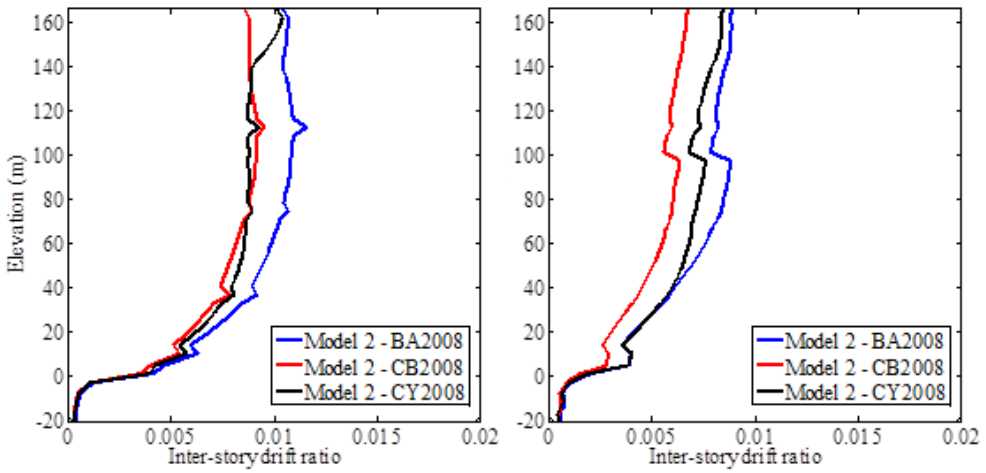

Figure 5.8. Mean IDR graphs for Model 2 with three different GMPEs in X and Y directions.

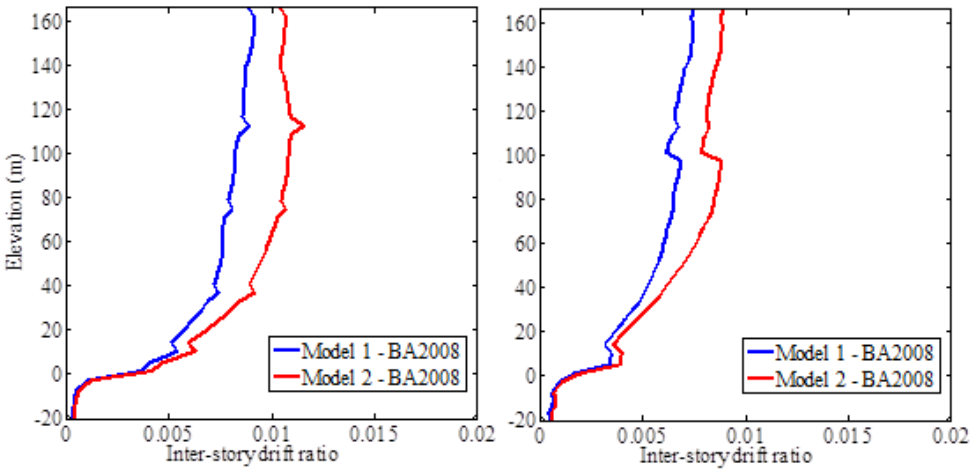

Figure 5.9. Mean IDR graphs for BA2008 using Model 1 and Model 2 in X and Y directions.

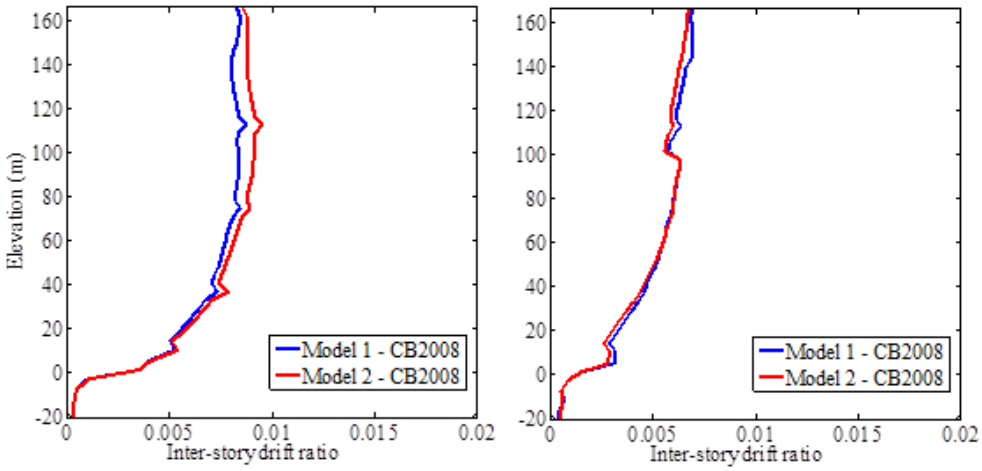

Figure 5.10. Mean IDR graphs for CB2008 using Model 1 and Model 2 in X and Y directions.

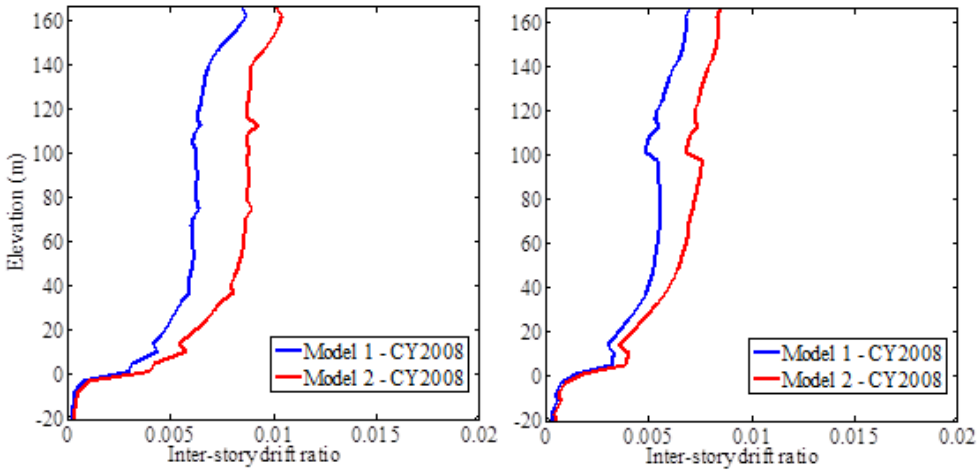

Figure 5.11. Mean IDR graphs for CY2008 using Model 1 and Model 2 in X and Y directions.

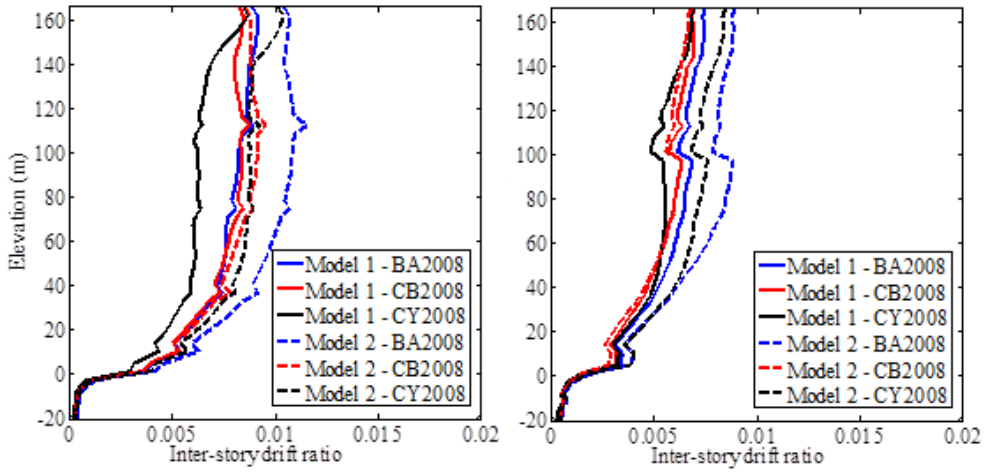

Figure 5.12. Mean IDR graphs for all sub-models in X and Y directions.

Table 5.1. Summary of maximum differences in inter-story drift ratio.

Uncertainty	**Fixed**	**Max. difference in X–direction (%)**	**Max. difference in Y–direction (%)**
GMPE	**Model 1**	38	42
	Model 2	26	41
Model	**BA2008**	33	31
	CB2008	10	13
	CY2008	49	48
Total		79	80

6. SUMMARY AND CONCLUSIONS

The uncertainties and their effects on seismic hazard estimations and the building response are investigated in this study. Two different seismic hazard models (regarding their recurrence characteristics) with three individual GMPE sets (per each) were defined. That is, 6 different combinations of recurrence models and GMPEs were utilized for selection of input ground motions, separately. In order to select the input ground motions, deaggregation analyses were performed so that the most contributing distance and magnitude pairs are determined. The selected ground motions were then scaled such that their mean acceleration response spectrum is above the uniform hazard spectrum in the period range of $0.2T_1$ - $1.5T_1$. The idea behind this is including the higher mode effects (by $0.2T_1$) and considering the period elongation due to yielding (by $1.5T_1$). Apart from that, a 43-story reinforced concrete tall building in Istanbul is instrumented and modeled. System identification techniques are utilized to validate the finite element model of the structure in order to represent the real case. By using the previously obtained input ground motions, linear time history analyses were conducted where the horizontal components of the earthquakes were acted simultaneously. The linear elastic inter-story drift ratios were adopted as the guiding parameter for the level of uncertainties. The main motivation of these steps is to reveal and understand the effect of the uncertainties of seismic hazard phase on the linear elastic response of the structure which had been instrumented and validated before. It is crucial to validate or update the FEM according to the system identification results in order to catch a realistic behavior of the real structure.

The uncertainties are classified as the ones originating from the recurrence characteristics, and from the selection of GMPEs. Their individual and combined effects on the response are evaluated separately. When the individual effect of the recurrence models is examined (Model 1 and Model 2), it was observed that the level of uncertainties depend on the employed GMPE. For example, when the Model 1 and the Model 2 are compared, the maximum of the difference in the IDRs among all storeys are 10%, 30%, and 50% (for both directions) for CB2008, BA2008, and CY2008, respectively.

When the individual effects of the GMPEs are considered, it was observed that the uncertainties are much less sensitive to the model selection. However, for the same models, the maximum differences among the GMPEs are about 40% in terms of inter-story ratios (for both directions).

Although the CY2008 tend to yield (almost 3 times that of the BA2008) higher spectral acceleration values in relatively low periods, for long periods such as 4 s spectral acceleration, which is the fundamental vibration period of the structure, the spectral acceleration values of CY2008 can drop to 2/3 of the BA2008. Therefore, considering all of the 6 possible combinations, the maximum difference can reach up to 80% which are the difference between the Model 1 – CY2008 (the minimum) combination and the Model 2 – BA2008 (the maximum) combination.

To sum up, according to the combined effects of the aforementioned reasons, the inter-story drift ratios (which can be a realistic representative of the damage) can exhibit significantly large uncertainties. This means that, the effect of the probabilistic seismic hazard on a tall building is highly susceptible to the earthquake recurrence models and the selection of the GMPEs. As a possible candidate for the solution of this problem, logic trees are utilized in practice. Although the logic tree is most widely accepted tool in dissolving aleatory uncertainties, it should be noted that, logic trees themselves are also comprised of subjective decisions in weighting phase.

As an extension to this study, effect of ε in input ground motion selection on response of a structure may be investigated. By introducing modeling uncertainties into study, a total probabilistic assessment of the structure from input to output and also capacity can be achieved, which would be an interesting study. Linear time-history analyses are conducted in this study due to time limitations, conducting nonlinear analyses would give more meaningful results which is the next objective of this study. Developing an original PSHA code which performs both PSHA and deaggregation would be a challenging goal which I want to achieve. In addition to these future plans, developing a real time monitoring system for the instrumented structure is also part of my future study plans.

REFERENCES

ACI Committee 318, 2008, "Building Code Requirements for Structural Concrete (ACI318-08) and Commentary", American Concrete Institute, Farmington Hills, MI.

Atkinson, G.M., and K., Goda, 2011, "Effects of Seismicity Models and New Ground-Motion Prediction Equations on Seismic Hazard Assessment for Four Canadian Cities", *Bulletin of the Seismological Society of America*, Vol. 101, No. 1, pp. 176–189, February 2011, doi: 10.1785/0120100093.

ASCE 7-05, "Minimum Design Loads for Buildings and Other Structures.", ASCE/SEI 7-05, Reston, VA.

Baker, J.W., 2008, " An Introduction to Probabilistic Seismic Hazard Analysis (PSHA)", White Paper, Version 1.3, 72 pp.

Baker, J.W., 2011, "Conditional Mean Spectrum: Tool for Ground-Motion Selection", *Journal of Structural Engineering*, 2011.137:322-331.

Baker, J.W., and C.A. Cornell, 2005, "AVector-Valued Ground Motion Intensity Measure Consisting of Spectral Acceleration and Epsilon", *Earthquake Engineering and Structural Dynamics*, 2005; 34:1193–1217

Baker, J.W., and C.A. Cornell, 2006, "Spectral Shape, Epsilon and Record Selection", *Earthquake Engineering and Structural Dynamics*, 2006; 35:1077-1095

Bazzurro, P., and C.A. Cornell, 1999, "Disaggregation of Seismic Hazard", *Bulletin of the Seismological Society of America*, 89, 2, pp. 501-520, April 1999.

Bommer, J.J., and N.A., Abrahamson, 2006, "Why Do Modern Probabilistic Seismic-Hazard Analyses Often Lead to Increased Hazard Estimates?", *Bulletin of the Seismological Society of America*, Vol. 96, No. 6, pp. 1967–1977, February 2006

Boore, D.M., and G.M. Atkinson, 2008, "Ground-Motion Prediction Equations for the Average Horizontal Component of PGA, PGV, and 5%-Damped PSA at Spectral Periods between 0.01 s and 10.0 s", *Earthquake Spectra*, Volume 24, No. 1, pages 99–138, February 2008; © 2008, Earthquake Engineering Research Institute.

Brincker, R., L., Zhang and P., Andersen, 2001, "Modal Identification of Output-Only Systems Using Frequency Domain Decomposition", *Smart Materials and Structures*, No. 12, pp. 441-445.

Brownjohn, J.M.W., T.C.,Pan and X.Y., Deng, 2000, "Correlating Dynamic Characteristics from Field Measurements and Numerical Analysis of a High-Rise Building", *Earthquake Engineering and Structural Dynamics*, No. 29, pp.523-543.

Campbell, K.W., and Y. Bozorgnia, 2008, "NGA Ground Motion Model for the Geometric Mean Horizontal Component of PGA, PGV, PGD and 5% Damped Linear Elastic Response Spectra for Periods Ranging from 0.01 to 10 s", *Earthquake Spectra*, Volume 24, No. 1, pages 139–171, February 2008; © 2008, Earthquake Engineering Research Institute.

Chiou, B.S.-J., and R.R. Youngs, 2008, "An NGA Model for the Average Horizontal Component of Peak Ground Motion and Response Spectra", *Earthquake Spectra*, Volume 24, No. 1, pages 173–215, February 2008; © 2008, Earthquake Engineering Research Institute.

Cramer, C.H., M.D. Petersen, and M.S. Reichle, 1996, "A Monte Carlo Approach in Estimating Uncertainty for a Seismic Hazard Assessment of Los Angeles, Ventura, and Orange Counties, California", *Bulletin of the Seismological Society of America*, Vol. 86, No. 6, pp. 1681–1691, December 2006.

Demircioğlu, M.B., 2010, "Earthquake Hazard and Risk Assessment for Turkey", PhD Thesis, Kandilli Observatory and Earethquake Research Institute, Bogazici University

Erdik, M., M. Demircioğlu, K. Şeşetyan, E. Durukal and B. Siyahi, 2004, "Earthquake Hazard in Marmara Region, Turkey", *Soil Dynamics and Earthquake Emgineering*, No. 24, pp. 605-631.

Gardner, J.K., and L. Knophoff, 1974, "Is the Sequence of Earthquakes in Southern California, with Aftershocks Removed, Poissonian?", *Bulletin of the Seismological Society of America*, Vol.64, No. 5, pp. 1363-1367, October 1974.

Goulet, C.A., C.B. Haselton, J. Mitrani-Reiser, J.L. Beck, G.G. Deierlein, K.A. Porter, and J.P. Stewart, 2007, "Evaluation of the Seismic Performance of a Code-Conforming Reinforced-Concrete Frame Building-from Seismic Hazard to Collapse Safety and Economic Losses", *Earthquake Engineering and Structural Dynamics*, 2007; 36:1973–1997.

Gutenberg, B. and C. F. Richter, 1954, "Seismicity of the Earth and Associated Phenomena" ,Princeton University Press, 2nd edition.

Gülkan, P., 2012, "Expecting the Expected: 1 g Peak Motions in the İstanbul Metropolitan Area", Proceedings of the 15th World Conference on Earthquake Engineering, September 24-28, Lisbon, Portugal, 2012.

Jalayer. F., I. Iervolino, and G. Manfredi, 2010, "Structural Modeling Uncertainties and Their Influence on Seismic Assessment of Existing RC Structures", *Structural Safety* 32 (2010) 220–228

Kalkan, E., P. Gülkan, N. Yılmaz, and M. Çelebi, 2009, "Reassessment of Probabilistic Seismic Hazard in the Marmara Region", *Bulletin of the Seismological Society of America*, Vol. 99, No. 4, pp. 2127–2146, August 2009, doi: 10.1785/0120080285.

McClusky, S., S. Balassanian, A. Barka,C. Demir,S. Ergintav,I. Georgiev,O. Gurkan,M. Hamburger,K. Hurst,H. Kahle,K. Kastens,G. Kekelidze,R. King,V. Kotzev,O. Lenk,S. Mahmoud,A. Mishin,M. Nadariya,A. Ouzounis,D. Paradissis,Y. Peter,M. Prilepin,R. Reilinger,I. Sanli,H. Seeger,A. Tealeb,M. N. Toksöz, and G. Veis, 2000, "Global Positioning System Constraints on Plate Kinematics and Dynamics in the Eastern Mediterranean and Caucasus", *Journal of Geophysical Research*, Vol. 105, pages 5695–5719.

McGuire, R.K., C.A. Cornell, and G.R Toro, 2005, "The Case for Using Mean Seismic Hazard", *Earthquake Spectra*, Volume 21, No. 3, pages 879-886, August 2005; © 2005, Earthquake Engineering Research Institute.

Moaveni, B., A.R. Barbosa, J.P. Conte, and F.M. Hemez, 2013, "Uncertainty Analysis of System Identification Results Obtained for a Seven-Story Building Slice Tested on the UCSD-NEES Shake Table", *Structural Control and Health Monitoring*.

Ordaz, M., F. Martinelli, A. Aguilar, J. Arboleda, C. Meletti, and V. D'Amico, 2014, "CRISIS", Institute of Engineering, UNAM, Mexico City, Mexico.

Parke J.R., T.A. Minshull and G. Andersen, 1999, "Active Faults in the Marmara Sea, Western Turkey, Imaged by Seismic Reflection Profiles", Terra Nova, 11, 223-227.

PEER Strong Motion Database, 2005, "The Pacific Earthquake Engineering Research", Center and the University of California.

Porter, K.A., J.L. Beck, and R.V. Shaikhutdinov, 2002, "Sensitivity of Building Loss Estimates to Major Uncertain Variables", *Earthquake Spectra*, Volume 18, No. 4, pages 719–743, November 2002; © 2002, Earthquake Engineering Research Institute.

Reasenberg, P., 1985, "Second-order Moment of Central California Seismicity, 1969-1982", *Journal of Geophysical Research*, Vol. 90, No. B7, pages 5479-55495, June 10, 1985

RETMC, Regional Earthquake-Tsunami Monitoring Center, Bogaziçi University, Kandilli Observatory and Earthquake Research Institute, accessed July 28, 2016, www.koeri.boun.edu.tr/sismo/2/earthquake-catalog/

Schwartz, D.P., and K.J. Coppersmith, 1984, "Fault Behavior and Characteristic Earthquakes: Examples From the Wasatch and San Andreas Fault Zones", *Journal of Geophysical Research*, Vol. 89, No. B7, pages 5681-5698, July 10, 1984

Skolnik, D., Y. Lei, E. Yu, J.W. Wallace, 2006, "Identification, Model Updating, and Response Prediction of an Instrumented 15-Story Steel-Frame Building", *Earthquake Spectra*, Volume 22, No. 3, pages 781–802, August 2006; © 2006, Earthquake Engineering Research Institute.

Smith, A. D., T. Taymaz, F. Oktay, H. Yuce, B. Alpar, H. Basaran, J. A. Jackson, S. Kara, and M. Simsek, 1995, "High-resolution seismic profiling in the Marmara Sea (Northwest Turkey); Late Quaternary sedimentation and sea-level changes", *Spec. Pap. Geol. Soc. Am.* 107, 923–936.

Stepp, J. C., 1973, "Analysis of Completeness of the Earthquake Sample in the Puget Sound Area", In: S.T. Handing (Editor), Contributions to Seismic Zoning. NOAA Tech. Report., ERL 267-ESL 30, U.S. Dep. of Commerce, USA.

Turkish Standards Institute, 2007, "Turkish Seismic Code", Ankara.

Turkish Standards Institute, "TS500 Building Code Requirements for Structural Concrete", Ankara.

Ventura, C.E., J.F. Lord, M. Turek, R. Brincker, P. Andersen, and E. Dascotte, 2005, "FEM Updating of Tall Buildings using Ambient Vibration Data", In C. Soize, & G. I. Schuëller (Eds.), Structural Dynamics EURODYN2005: Proceedings of 6th International Conference on Structural Dynamics, Paris, France, 4-7 September 2005. (pp. 237-242). Millpress.

Weichert, D.H., 1980, "Estimation of the Earthquake Recurrence Parameters for Unequal Observation Periods for Different Magnitudes", *Bulletin of the Seismological Society of America*, Vol. 70, No. 4, pp. 1337-1346, August 1980.

Wells, D.L., and K.J. Coppersmith, 1994, "New Empirical Relationships Among Magnitude, Rupture Length, Rupture Width, Rupture Area, and Surface Displacement", *Bulletin of the Seismological Society of America*, Vol. 84, No. 4, pp. 974–1002, August 1994.

Youngs, R.R., and K.J. Coppersmith, 1985. "Implications of Fault Slip Rates and Earthquake Recurrence Models to Probabilistic Seismic Hazard Estimates", *Bulletin of the Seismological Society of America*, Vol. 75, No. 4, pp. 939-964, August 1985.

Yunatci, A.A., and K.Ö. Çetin, 2006, "Impact of attenuation models on probabilistic seismic hazard analysis: A case study for Bursa City, Turkey.", Proceedings of the 8th U.S. National Conference on Earthquake Engineering, April 18-22, San Francisco, California, USA, 2006.